Computing with Self-Excitatory Cliques: A Model and An Application to Hyperacuity-scale Computation in Visual Cortex

Douglas A. Miller*
Steven W. Zucker†
Center for Computational Vision and Control
Depts. of Computer Science and Electrical Engineering
Yale University
P. O. Box 208285, New Haven, CT U.S.A.
steven.zucker@yale.edu

TO APPEAR IN *Neural Computation*, **11**(1), 1999

Abstract

We present a model of visual computation based on tightly inter-connected cliques of pyramidal cells. It leads to a formal theory of cell assemblies, a specific relationship between correlated firing patterns and abstract functionality, and a direct calculation relating estimates of cortical cell counts to orientation hyperacuity. Our network architecture is unique in that (1) it supports a mode of computation which is both reliabile and efficent; (2) the current-spike relations are modeled as an analog dynamical system in which the requisite computations can take place on the time scale required for an early stage of visual processing; and (3) the dynamics are triggered by the spatio-temporal response of cortical cells. This final point could explain why moving stimuli improve vernier sensitivity.

1 Introduction

Consider a region of our visual field innervating a patch of primary visual cortex a few mm on a side, containing, say, 10^6 mostly mutually excitatory neurons. Does it make sense to

*Douglas A. Miller, formerly of the Center for Intelligent Machines, McGill University, Montreal, Canada, passed away in 1994. This article is derived from "A Model of Hyperacuity-scale Computation in Visual Cortex by Self-excitatory Cliques of Pyramidal Cells", TR-CIM-93-12, August 1993. Portions were also presented at the Workshop on Computational Neuroscience, Marine Biological Laboratories, Woods Hole, MA, in August, 1993.

†Research supported by AFOSR, NSF, NSERC, and Yale University.

talk about this small patch of cortex as a basic unit of our visual system, and, if so, how crude is it? For example, how many distinct lines could *just this one patch of cortex* reliably represent? We suggest that knowing whether the biggest possible number is 10, 10^4 or 10^7 is critical to the understanding of our visual system, because to determine this number we must address how this unit of cortex is functioning. Thus our main goal in this paper is to develop a model of computation sufficiently biological to apply to this patch of cortex, but which can also be viewed as an abstract model of computational vision which can represent lines. To reduce this goal to manageable proportions, we focus on the representation of orientation for short line segments.

The choice of studying the representation of short line segments was made for several reasons. To begin, we are developing a theory of visual information processing based on tangents to image curves (Zucker et al, 1989). The concrete realization of these tangents is short oriented segments, the natural limit to which is given by orientation hyperacuity (Westheimer, 1990). However, while most neurons in visual cortex are orientation selective, their tuning is broad (± 7.5 deg in monkeys before significant falloff). Even the smallest receptive fields are $\geq$ 12 arc min^2 on average in monkeys and humans (Hubel and Wiesel 1968, Wilson et al. 1990). These facts stand in crude comparison with the precision of hyperacuity involving contours with widths of about 1 arc min. Thus our second motivation is to understand how this (and only this) precise level of functional performance can be achieved with coarse units.

Such questions raise the more general one: Are individual neurons the natural basis for expressing visual computations, or are visual computations most naturally expressed at the circuit level? We derive the surprising result that, according to our model, a circuit structure can take processing elements (neurons) which by themselves are both extremely crude and highly unreliable, and create aggregate units which are *both* extremely precise and highly reliable. This result specifies a type of *cell assembly* very much in the spirit of Hebb's (1949) original proposal, and those of Braitenberg (1974, 1978, 1985; Braitenberg and Schuez, 1991) and Palm (1980; 1982; 1993; Palm and Aertsen, 1986); Wennekers et al, 1995. Nevertheless, there are important technical differences from these earlier works. We consider analog neural models, while Braitenberg, Palm, Aertsen etc. consider spiking ones. (The relevant issues of time constants are discussed later.)

The particular type of cell assembly we are postulating is illustrated in Fig. 1, where a circuit of cells with approximately (but not exactly) the same spatio-temporal and orientation selectivities form a clique whose composite response is of fundamental interest. Thus our model postulates a level of organization among neurons more precise than single-cell receptive field properties (more below), and it provides a formal bridge between spike train distributions and abstract function (cf. [(cf. Softky and Koch, 1992; Tsodyks et al, 1993]). Most importantly, our model differs in fundamental ways from previous attempts to construct reliable systems from unreliable components. In particular, Moore and Shannon (1956) developed the foundations of highly redundant recursive systems, but these seem unsuitable for biology because the redundant circuitry is largely a sink for energy without providing any interim benefit. Our third motivation, then, is to seek architectures that achieve reliability without wasted redundancy. In particular we will show how, in our parallel analog model of computation, the extra number of processors needed to achieve reliability *at the same time* increases the information content of the system (cf. Winograd and Cowan 1963, Barlow

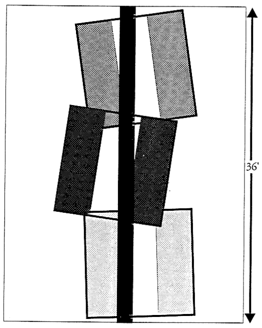

Figure 1: Receptive fields for representing a thin line contour. A white slit contour stimulus about 1.5 arc min width (heavy black outline) excites a highly interconnected clique of cortical S cells, whose receptive fields are represented here by (12 arc min)^2 rectangles, to maximal saturated feedback response by crossing, in the appropriate direction and within a narrow time interval, the edge response region (cf. Fig. 4) of a sufficiently large proportion of the clique's cells. Three such receptive fields, forming part of a larger clique, are illustrated here. According to the theory proposed in the text, a small change in orientation of the contour will cause a modest decrease in the probability of an initial spike from the cells in the clique that would be sufficient to prevent a saturated feedback response from the clique as a whole.

1983).

The key ideas behind our model and the corresponding mode of computation, are, first, the idea of groups of tightly interconnected excitatory neurons capable of bringing themselves to saturation feedback response following a modest initial afferent bias current, rather like a match igniting a conflagration, to borrow a simile from Douglas and Martin (1992). We call these groups *cliques*. [1] Secondly these cliques of neurons, although there may be an extremely large number of them, are themselves relatively small, consisting of perhaps a few dozen excitatory pyramidal cells with certain characteristics (see below). On the other hand an individual such cell may simultaneously belong to hundreds of different cliques, and therein lies the system's ability to reliably store and retrieve large quantities of information with highly unreliable processing elements. We schematically illustrate the basic retrieval computation in Fig. [2].

The assumption that excitatory groups of neurons exist is based on the following facts (see also Douglas et al., 1995):

[1] *Clique* in directed graph theory refers to a subset of nodes (neurons, in this case) which is completely interconnected, that is, having an arc (synapse) from each node to each other node. We note that such a perfect arrangement is unlikely in biology, and indeed subsets of neurons which are merely interconnected to a sufficiently high degree are sufficient for our analysis (cf. Section 3.1). Thus we will use *clique* to refer to either kind of set, and assume that the exact meaning will be made clear from context. Braitenberg (1985) stressed the role of synchronous firing in establishing such connections.

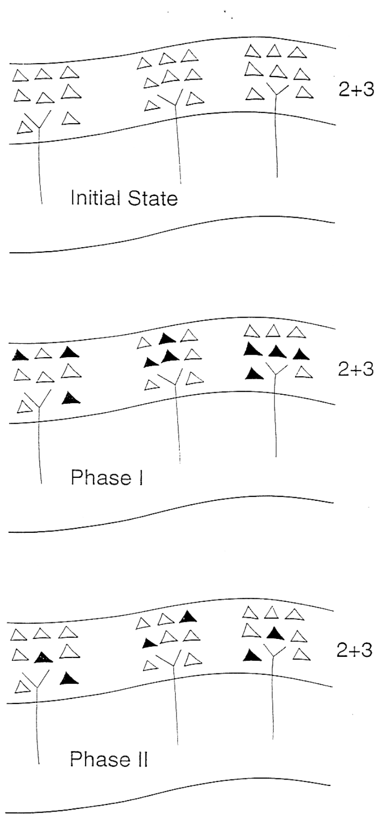

Figure 2: A schematic illustration of the two phases of the computation for activating a cortical clique. The model is sketched in terms of layer 2/3 pyramidal S cells, for reasons developed in the text. (*Top*) Prior to Phase I the layer 2/3 pyramidal cells in a patch of cortex are initially largely quiescent, corresponding to an initial state for the computation. Among these hundreds of thousands of cells are several times that number of cortical *cliques* each containing about 33 highly interconnected cells. A "computation" amounts to activating the cells in a single clique, but no others, to saturation feedback response levels. (*Middle*) In the beginning of Phase I, afferent stimulation, either directly or indirectly (e.g., from the LGN), produces a single spike in a majority of the cells (filled) in one clique (whose cells can be distributed among many different iso-orientation areas, including the three illustrated), as well as a certain number of other cells (also filled) outside the clique (noise). (*Bottom*) Because the clique has a sufficient level of excitatory interconnections, all its cells (filled) drive themselves, as part of an analog dynamical system (cf. Fig. 7), to saturation response levels of about 5 spikes in 25 msec (end of Phase I), whereas the initially activated cells outside the clique (now open) ultimately return to their resting membrane potentials and do not spike further (end of Phase II). Thus the clique has been "retrieved" through a parallel analog computation, and during this 25 msec period is available as input for further processing in the cortex or elsewhere. Adaptive spiking properties of pyramidal cells (cf. Figs. 2 and 7, *top*), possibly combined with general inhibitory mechanisms, terminate the computation, and return the system to the initial quiescent state.

1. Most connections are from spiny excitatory cortical cells to other spiny excitatory cortical cells within a few millimeters horizontal distance (Douglas and Martin 1990).

2. Most, if not all, direct afferents from the lateral geniculate nucleus are excitatory. (Bishop et al. 1973, Ferster and Lindström 1983, Douglas and Martin 1992).

3. Inhibition is much less specific than excitation, both temporally and spatially, and is additive, not multiplicative (Bishop et al. 1973, Douglas et al. 1988).

4. Most excitatory connections from layer 2/3 pyramidal cells are to other layer 2/3 or possibly layer 5 pyramidal cells with about the same orientation specificity (Rockland and Lund 1982, 1983; Rockland et al. 1982; Gilbert and Wiesel 1983,1989; Callaway and Katz 1990).

5. Most, if not all, connections in visual cortex undergoing long-term potentiation and depression ("Hebbian learning") are between spiny excitatory cells (Artola et al. 1990, Douglas and Martin 1990). (This point is also important for learning cliques, which we shall not discuss in this paper.)

In addition to these structural features, two aspects of neuronal dynamics are central to our model of computing with cliques. First, we note that most excitatory cortical cells exhibit a typical "regular spiking" behavior (McCormick et al. 1985, Douglas and Martin 1990), which adapts within a 25 msec period from an initial high spiking rate (e.g. 300 Hz) to a much lower sustained rate (Fig. 3). We shall take this initial higher rate of activity as fundamental, and shall use it to carry the relevant information. In particular, the "conflagration" referred to earlier will be carried by short bursts of rapid activity for all neurons within a clique. This also implies that the time scale for a computation should be around 25 msec, a time scale that is relevant for cortical computations in V1 given that total processing can occur within 200 msec. Diffuse inhibition then returns the system to base state.

Heller et al (1995), in an attempt to characterize the information transmitted about visual patterns as a function of time found, in visual cortex, that 25 ms. emerged as a critical interval. This empirical finding agrees with the above observations.

The second dynamical aspect of our model derives from the observation that, whereas orientation sensitivity is crude, spatio-temporal precision in response to *moving edges* is high for a large class of cortical cells (Bishop et al. 1971, 1972, 1973; Schiller et al. 1976a,b,c; Henry 1977). Henry (1977) called these S cells, and we shall take an abstraction of them as the basic neural unit for our clique-based computation. It is this specificity that will provide the necessary timing to ignite the "conflagration."

The S cell category is derived from the Hubel and Wiesel (1962, 1968) simple cell, but is different in that its response is based primarily on moving edges. In particular, the S cell, while often (but not always) having distinct stationary ON/OFF response zones, does not respond to *moving* contour stimuli with additive summation in the direction perpendicular to orientation, nor does it tend to exhibit antagonism between the ON/OFF regions for such stimuli. Furthermore its response zones to moving contours can not in general be predicted more than very approximately from the location of any classic ON/OFF zones it may have

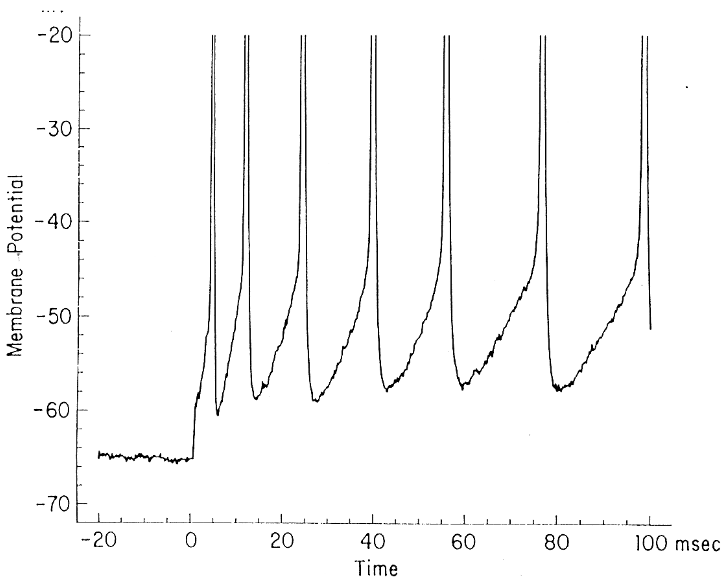

Figure 3: The spike train of a regular spiking cortical neuron under constant .6 nA current stimulation. Cell was recorded from layer 5 of rat visual cortex, in vitro. Note the characteristic rapid transient and subsequent decrease in the firing rate to mean level (cf. Fig. 7, *top*). (Data kindly supplied by R. Douglas.)

(Bishop et al. 1972; see discussion, Bishop et al. 1973, P. 58). In addition the direction selectivity of response can differ from what would be predicted from the Hubel and Wiesel criteria for simple cells (Hubel and Wiesel 1962). Rather when spontaneous activity is artificially enhanced, or exists naturally at an exceptionally high level, well-defined response peaks tend to appear in both directions of motion for both light and dark edges. [2] (Bishop et al. 1973, Fig. 1, Schiller et al. 1976a, Fig. 14A). Such an S-cell response histogram is given in Fig. 4. Furthermore within broad limits the spatial location of S-cell edge responses appear to be independent of contour velocity (Bishop et al. 1971, Figs. 5 and 6). In the absence of natural or artificial spontaneous firing, an S-cell typically responds to only certain edges and directions of motion.

The spatio-temporal precision of S-cells differs from the "average firing rate" class of codes normally considered. This raises the question of whether the retina or the LGN are capable of providing a cohort of spikes sufficently close (in time) to start the process we are studying. While the question is still open experimentally, recent retinal analyses are suggesting that such information may well be available in synchronous spike distributions (Meister, 1996). Indirect evidence for this has been in the literature for some time (Victor, 1987). Research in the LGN also has uncovered quite a bit of information in spike timing (e.g., McClurkin et al, 1991). Finally we note that another coding scheme (different from

[2]A light edge is one whose light portion is increasing, and a dark edge is one whose dark portion is increasing. Thus the same instantaneous visual configuration can be a light or dark edge depending on its direction of motion.

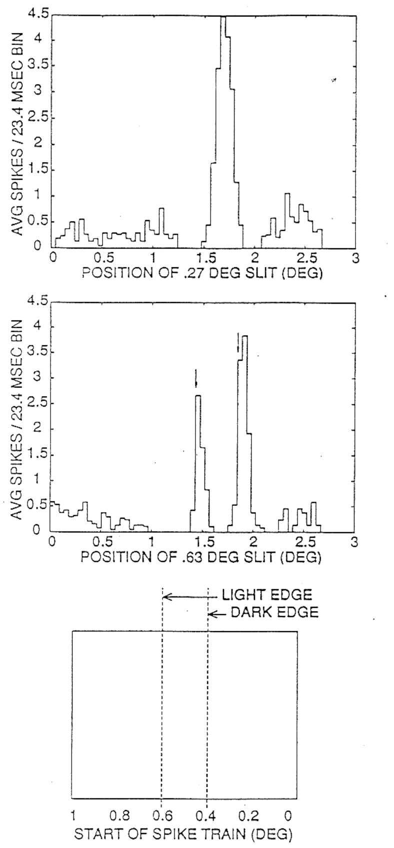

Figure 4: Neuronal response to a narrow slit of light is a composition of separate finely-tuned responses to each of its two edges. (*Top*) A response histogram for an S cell from parafoveal primary visual cortex of a macaque monkey, for twenty passes of a .27 deg slit of light from right to left visual field at a velocity of 2 deg/sec. Histogram is from left to right with time, and for each pass, each bin counts spikes over a period of 23.4 msec and corresponds to a stimulus movement of .046 deg. (*Middle*) Same as above, but with slit width of .63 deg. Two separate peak responses appear, consistent with the hypothesis that the cell is responding separately to the leading (light) and trailing (dark) edge of the slit. Separation of the peaks is about .21 deg less than the separation of the slit, which Schiller et al. (1976a) interpret as meaning that the light and dark edge response regions are separated by about that much, with the light edge response region to the left in the visual field of that for the dark edge. This cell had an exceptionally high spontaneous activity level, and therefore one can observe sideband inhibition caused by the stimuli in both *top* and *middle* (zero-level portion at extreme right of both graphs is not part of data). Two vertical arrows in bottom graph indicate the beginning of the kind of sudden response onset predicted by our theory. The 25 msec spike train described in the text could be expected to fall within two bins. Note that the two adjacent bins beginning with the first arrow represent an average response of 4.3 spikes, and the two adjacent bins beginning with second arrow represent an average response of 7.2 spikes. (*Bottom*) Spatio-temporal receptive field positions of the edges signaled by the beginnings of the spike trains described above. Light edge location is indicated by 4.3 spikes on average, dark edge by 7.2 spikes. (Histograms redrawn from Schiller et al. 1976a).

ours) has recently been proposed that is also triggered by rapid spikes (doublets); see Traub, Whittington, Stanford, and Jefferys (1996).

The clique, then, will consist of a collection of S-cells scattered slightly in position and orientation (Fig. 1).

We note that this mode of computation amounts (cf. Georgopoulos et al. 1989, Gilbert and Wiesel 1990, Lehky and Sejnowski 1990) to a distributed code for hyperacuity, but several critical features distinguish it from other distributed code models. In particular there is no population averaging. *The fact that a highly specific visual event has occurred at a specific time is announced to the rest of the brain by the (roughly) simultaneous saturation-level activation of a few dozen normally quiescent cells in primary visual cortex.* In particular, one does not need to measure the time intervals of the spike trains which are produced, or find a higher-level cell to average the response histograms of the cells which are spiking. Rather it is the fact that a particular clique of cells are firing at saturation levels which is the crucial piece of information being conveyed. While others have stressed the possibilities of coincident firing (e.g., Abeles, 1991), a major aspect of the present work lies in demonstrating, via a combination of existing empirical data and mathematical and probabilistic analysis, that a primate's primary visual cortex is capable of storing a sufficient number of self-excitatory cliques (and hence this information) to constitute a hyperacuity-scale representation of the external visual world. Thus, while our model is in the spirit of those that attempt to solve "binding" problems by a form of synchrony (for a review, see Konig and Engel, 1995), the proposal is substantially more concrete.

There are two limits which come into play. One is the sheer number of cells, particularly the adaptive or *regular* spiking (McCormick et al. 1985) orientation selective pyramidal S and S_H cells (Henry 1977) [3] which are the predominant type in layers 2/3 in cats (Henry et al. 1979, Martin 1984) and a major if not predominant type in layers 2/3 in monkeys (Schiller et al. 1976a; see discussion, Section 2.2). The other limit is the temporal/spatial resolution of these cells (Bishop et al. 1971, 1972, 1973; Schiller et al. 1976a,b,c; cf. Fig. 4). We shall show that by increasing the numbers of such cells, one can make optimal use of this resolution, resulting in the potential for hyperacuity-scale performance. Thus we can view hyperacuity as the end result of what is available from optics, the physiology of neurons, the amount of brain tissue we can support, and the need for high resolution vision.

The remainder of this paper is organized in three sections. In Section 2 we develop our model informally, concentrating on its physiological interpretation and justification. Section 3 is mathematical. There we state our model precisely, and prove several of its key properties. In particular Proposition 1, Section 3.1, describes the dynamic behavior properties of a system of excitatory neurons modeled as a dynamical system of analog voltage amplifiers (cf. Hopfield 1984 and Fig. 7). In particular, for the latter system, an arbitrarily small output from a sufficiently large proportion of cells will drive the entire group of cells to saturation response. In a clique of real neurons, we argue that this corresponds to the case of a significantly large proportion of a group of highly interconnected cells receiving single-spike lower level afferent stimulation, thus driving the entire group to saturation firing.

Proposition 2, Section 3.1, is a technical result used in our calculation (done in Section 3.2) of the number of storable cliques of cells, and the amount of tolerable input noise (cf.

[3]The S_H cell is an endstopped S cell. Hereafter we shall generally include S_H cells in the S category.

Fig. 8 and Section 3.2). In addition we rigorously define in this section the key notions of *self-excitatory set*, *minimal* self-excitatory set, and *clique*. We then provide several applications of the model. An important result of the next section is the calculation of a cortical packing density for layer 2/3 S-type pyramidal cells which would be necessary and sufficient for observed orientation hyperacuity data in humans. The cell density calculated turns out to be very close to that observed for macaque monkeys. Following the discussion we also include an Appendix containing a glossary of symbols.

2 A Clique-based Model of Cortical Computation

Let us describe in more detail our analog network model for intrinsic horizontal connections in a small patch of primary visual cortex (an exact mathematical description is given in Section 3). Note, in particular, how it differs from the input/output view of controlled amplification proposed in Douglas et al., 1995.

Our cortical computational model supposes that we start from a stable reference state in which all or most neurons are quiescent, and then activate a relatively small number of them. Thus our model stores states as highly interconnected self-excitatory cliques of neurons (represented by voltage amplifiers), where activation of some proportion greater than half of the clique members beyond a certain moderate level fully activates the entire clique. There are two phases to this procedure, corresponding to two computations by the network. In the first phase, all input amplifiers are activated at some moderate level by a fixed set of input biases. Those amplifiers undergoing self-excitatory feedback then drive to their saturation values. In the second phase, the input biases are removed and all amplifier responses not undergoing feedback excitation decay out. We illustrate this process schematically in Fig. 2.

This two-phase computational model becomes relevant to the visual cortex by considering a 25 msec computational time frame, and the phenomenon of regular adaptive spiking to constant input current (McCormick et al. 1985, Douglas and Martin 1990), which can be understood in terms of cell membrane properties (McCormick 1990). Thus a moderately stimulated cell would be likely to produce no more than a single spike in a 25 msec interval (Fig. 7, *top*, responses for .3 to .6 nA), but one that is fully excited (1.5 nA) could produce about five (cf. also McCormick et al. 1985, Fig. 1). Since a cortical somatic time constant is typically much larger than the intervals we shall be concentrating on (as described below, 3.5 msec as compared with the 10-20 msec time constant [Douglas and Martin 1991]), we may assume an approximately linear current-voltage relation, and thus model a clique of these cells with a clique of voltage amplifiers with the same shape input/output function.

We presume that under either direct or indirect afferent stimulation there is sufficient input current arriving at a given target cell to produce a single spike (Fig. 2, *middle*). For members of a clique this will produce a large number of additional excitatory post-synaptic potentials within a few msec (Fig. 2, *bottom*), thus producing more spikes in these same cells, and any others in the clique, and bringing current input to these cells to saturation levels, as in the higher abscissa values in Fig. 7, *middle*. This chain of events will happen if and only if the initial proportion of activated clique members is sufficiently large. We model this dynamic ensemble feedback process among excitatory neurons with piecewise-linear voltage amplifiers (Fig. 7, *bottom*).

During this 25 msec computation, the mild additive feedback inhibition which appears to be an intrinsic part of the visual cortex (Douglas et al. 1988, 1989) could suppress any tendency of a nonclique cell receiving little or no excitatory feedback to respond more than once in the interval, but would be ineffective against clique cells undergoing short-term feedback excitation. In effect the inhibition would sharpen the distinction between the two classes of cells and reduce noise. The first class of cells could be regarded as undergoing an imprecise decaying input current, the second a highly precise, mutually activating response (Fig. 2, *middle* and *bottom*). In addition (or alternately) inhibition could serve to deactivate the system following a given computation, thus setting the stage for the next one, or allowing the same cells to represent other (e.g., downflowing) information in a separate time regime.

As we show elsewhere (Miller and Zucker 1998), the end results of both phases can be computed in a number of computational steps which is polynomial in the number of bits needed to specify the problem (as defined in Section 3). This can be done by a type of algorithm which we have described previously (Miller and Zucker 1991, 1992), and which is closely related to the well known simplex method for linear programming. What this analysis shows is that the problem of retrieving information within our cortical model is not in the class of computationally hard problems such as the traveling salesman (Hopfield and Tank 1985) for which no such algorithm is likely to exist (Garey and Johnson 1979). Knowing that a fundamental computation is performable in polynomial time would appear to be a distinct advantage in modeling systems on the scale of the visual cortex.

Two points should be stressed. First, the relative smallness (sparsity) of these cliques and the relatively small number of afferents which may be active at any given time is critical, both in order to obtain sufficiently many cliques to represent line contours on hyperacuity levels (one contour per clique), and in order for the computation not to end up activating the wrong cliques, or, at the extreme, producing a catastrophic epileptic response among the entire cell population.

Second, the specificity of response of an individual S cell to a moving edge contour need only be probabilistic. That is, given our clique model, for the entire clique to fire reliably when the contour is in a specific location and not otherwise, it is only necessary that the individual neurons composing the clique have a modest increase or decrease, respectively, in their individual *probabilities* of firing. Sufficient probabilities for the model we shall derive are given in Fig. 5.

We now describe some of the principal neurophysiological assumptions of our cortical model, and describe how these assumptions are justified by empirical evidence.

The first assumption is to limit a priori the possible number of input units which can be activated. This is consistent with our knowledge of cells in the visual cortex, where investigators often find it difficult to find any stimulus which will make a given neuron respond, and where there is in general an extremely low level of intrinsic activity (cf. Bishop et al. 1971, 1973; Schiller et al 1976a,b,c). Thus while it may seem strange at first to suppose a model of cortical computation, as ours is, based primarily on excitation, the reason a model of excitatory computation is possible *in the cortex* is because there has already been

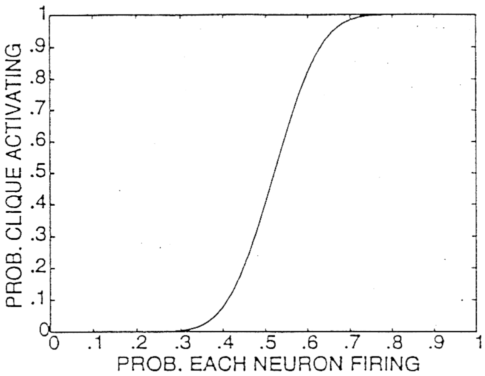

Figure 5: Probability of an entire clique firing as a function of the probability of its individual neurons firing. In this idealized case, all neurons have the same independent probability p (abscissa) of an initial spike within a given time interval. Assumed clique size is 33, and at least 17 neurons firing are assumed necessary for activation of the clique. The steep sigmoid curve implies that the reliability of the clique is virtually perfect even if individual neurons fire with .3 probability when they should not, and only .75 probability when they should (The computation is based on the 17-out-of-33 system discussed in Sec. 5).

a tremendous amount of filtering in the visual system prior to reaching this stage. Perhaps LGN feedback is involved in this filtering as well.

We may observe the vast contrast between this assumption and that of the Hopfield (1982) discrete model, in which a randomly chosen storage state is as likely to have as many *on* as *off* states, and the Hopfield (1984) analog model where *all* the neurons are potentially firing. This assumption is untenable in the visual cortex, not only because cortical neurons are typically quiescent, but because, even if they all could be firing, their average spike rates of 100 Hz and less could not specify the interior state or trajectory of an analog dynamical system with anything approaching the precision which Hopfield's system seems to demand. However, versions of analog neural network models which are both biologically and computationally plausible are possible, and we have described broad classes of such models in previous work (Miller and Zucker 1991, 1992). The present paper may be viewed as an application of this work to the visual cortex.

Along these lines, we should note that the information-theoretic efficiency of sparse input *discrete* associative and auto-associative networks with large numbers of computing elements has been known for some time [Willshaw et al. (1969), Willshaw and Longuet-Higgens (1970), Palm (1981), Amit et al. (1987), Amari (1989), Amit (1989)]. Roughly speaking we are extending these discrete sparse-input models to the analog case. We thereby derive a greater biological realism, firstly with regard to variable spiking rates and capacitive time constants, and also with regard to the distinction between average and *saturation* firing rates (cf. Figs. 2 and 7). This latter point arises only when considering visual representations through tightly interconnected, self-excitatory cliques of neurons. In addition such representations permit a number of additional random noisy inputs many times larger than the number of cells which would ultimately be responding at saturation (cf. Fig. 8, *bottom*).

Our second assumption (also a basis for the sparse-discrete models cited above) is that all recurrent connections (synapses) are only capable of being modified within the same sign, i.e. excitatory (see also Abeles (1991). This assumption is based on the prevalence of glutamergic excitatory connections in the neocortex (Douglas and Martin 1990), as well as the evidence for NMDA receptor-based long-term potentiation and depression in the primary visual cortex (Artola et al. 1990, Singer 1990), particularly during the critical period. These receptors are found primarily on dentritic spines, which are the major sites of excitatory input to excitatory cells in the neocortex (Douglas and Martin 1990). The most dramatic evidence, however, is morphological, since one can literally view the pruning and growth of excitatory pyramidal-pyramidal connections in cat area 17 in the first 6 postnatal weeks (Callaway and Katz 1990).

Our third assumption, which amounts to saying that a patch of cells in layers 2/3 can be reasonably modeled as though it were a continuous or *analog* dynamical system (cf. Hopfield 1984, Cohen and Grossberg 1983, Sejnowski 1981), is treated in the following section; see also Bopalsamy and He (1994), Marcus and Westervelt (1989), Marcus et al (1990), Waugh et al (1991); for different approaches to such modeling see: Abbott (1993), Harth et al (1970), Nelken (1988), and Treves (1993).

Let us consider here, however, whether the inputs to this system can be viewed purely as a bias applied to a quiescent or *off* state of the system. This assumption is suggested by both the limited analog information storage capacity of cortical neurons (e.g. in the form of average membrane potential) and the growing body of empirical evidence that specific cortical populations respond to specific visual imputs with self-imposed correlations due to mutual feedback excitation combined with mild local inhibitory feedback within periods of 25 msec and less. (Cf. "cortical oscillations" for cats [Eckhorn et al. 1988, Gray and Singer 1989, Gray et al. 1989], "spatio-temporal distributions" for monkeys [Krüger and Becker 1991], and cortical feedback circuits [Douglas et al. 1988, 1989; Douglas and Martin 1990, 1992; see especially Douglas et al., 1995].) Thus a fundamental lack of short-term precision, and a lack of time for any kind of smoothing integration, argue against a dynamic model in which a well-defined trajectory takes us from a specific interior state to a final computed state, as one finds for example in Hopfield (1984), Hopfield and Tank (1985), and Hummel and Zucker (1983).

Finally there is the question of the excitatory cliques themselves – which we may regard as our fourth assumption. The existence of a large number of small subnetworks of cells which are tightly interconnected is consistent with our prior assumptions if we are interested in large-scale efficient storage of information. But what independent evidence is there for such kinds of connectivity? In fact it is here that we have the most striking empirical evidence of all, which becomes apparent once we consider the precise "information" which we want to store.

It is well known that, at a coarse resolution, there is a (piecewise) continuous topographical map of visual inputs in the cortex for orientation, ocular dominance, and location of receptive fields. However if we look more closely, there is within this globally orderly situation a tremendous amount of local randomness. From Hubel and Wiesel (1962, 1968, 1977) and Albus (1975, Part I), we see that (for monkeys and cats) there is a variance ("radial scatter") in the receptive field location of a cell at a given cortical point. Furthermore, as observed in cats (Albus 1975, Part II), while the mean orientation may progress continuously across iso-orientation bands, there is at any given point a considerable random variation imposed on the mean selectivity of a given cell. Thus a given oriented contour in the visual field (Fig. 1) will in all likelihood simultaneously innervate multiple neurons in several locations with about the same orientation preference. This observation has been supported and extended by later ones of Rockland and Lund (1982) and Rockland et al. (1982) in tree shrews, Rockland and Lund (1983) in monkeys, and Gilbert and Wiesel (1983, 1989) (also in cats) that layer 2/3 pyramidal cells in neighboring iso-orientation columns connect primarily to each other (Fig. 2). The improved sensitivity of a group of cells was also noted by Lehky and Sejnowski (1990) for stereo.

Finally, in closing the informal portion of the paper we observe that "computational analysis" in the sense popularly used in the neurobiological community has largely come to mean computer simulation of the behaving organism of one kind or another, either on a compartmental scale of individual neurons (e.g. Segev et al. 1989, Douglas and Martin 1992) or on a compartmental scale of relatively small networks of neurons (Wörgötter and Koch 1991), or large-scale simulations that do not attempt to model individual neurons (e.g. Miller et al. 1989). This paper is significantly different from these in that we use a purely mathematical *analysis* of systems of individual cells in the visual cortex, rather than computer simulation, to derive results on the behavior of numbers of cells on the order of 10^6, and synapses on the order of 10^{10}, which are typical numbers for a small patch of cortex. While not wishing to downplay the importance of simulation, we believe that at this stage in the development of our knowledge of the cortical visual system, a global analytic theory is badly needed, and it is this large gap which we are attempting at least partially to fill. In the context of existing neural models, ours may be viewed as combining an analog dynamical system model of the type popularized by Hopfield (1984) and the canonical cortical circuit of Douglas et al. (1989) (cf. also Douglas and Martin 1990, 1992). Roughly speaking, our model makes the former much more biological, and the latter much more specific, at least with regard to layer 2/3 of primary visual cortex. Finally, we repeat that it suggests a dynamics very different from the (constrained) gradient descent normally employed in neural networks (cf. Hummel and Zucker, 1983; Hopfield, 1984).

3 A Mathematical Description of the Model

3.1 Self-Excitatory Sets

We have described in a previous paper (Miller and Zucker 1992) a version of the well known recurrent analog network discussed in Hopfield (1984) with continuous piecewise-linear amplifiers rather than smooth sigmoids. We showed that the relative simplicity of this version can be useful in computational analysis, while not reducing the plausibility of the model with respect to real neurons. In fact as we have already implied in Fig. 7, *bottom*, piecewise-linear amplifiers are in general much *more* realistic than smooth sigmoids for empirically-based input-output relations at the neuronal level (cf. also McCormick et al. 1985, Calvin 1978).

This is hardly surprising since for all practical purposes they are a much more general class of functions (see Miller and Zucker 1992, Fig. 6).

We shall continue using this kind of analog network here, and familiarity with our earlier paper is helpful. Let u_i and V_i be interpreted as the input and output voltages of the (instantaneous) amplifier i described by a monotonically increasing piecewise-linear function $g_i(u_i) : [\alpha_i, \beta_i] \rightarrow \mathbf{R}$ given by

$$g_i(u_i) = \begin{cases} 0 & u_i < \alpha_{i,1} \\ \gamma_{i,1} u_i + \delta_{i,1} & \alpha_{i,1} \leq u_i \leq \beta_{i,1} \\ & \vdots \\ \gamma_{i,\omega(i)} u_i + \delta_{i,\omega(i)} & \alpha_{i,\omega(i)} \leq u_i \leq \beta_{i,\omega(i)} \\ 1 & u_i > \beta_{i,\omega(i)} \end{cases} \tag{1}$$

where

$$\alpha_i < \alpha_{i,1} < \beta_{i,1} = \alpha_{i,2} < \cdots < \alpha_{i,\omega(i)} < \beta_{i,\omega(i)} < \beta_i$$

and

$$\begin{aligned} \gamma_{i,k} &= [g_i(\beta_{i,k}) - g_i(\alpha_{i,k})]/[\beta_{i,k} - \alpha_{i,k}] \\ \delta_{i,k} &= g_i(\alpha_{i,k}) - \gamma_{i,k}\alpha_{i,k} \end{aligned}$$

for all integers k, $1 \leq k \leq \omega(i)$. (ω is an index for the piecewise-linear slope component of amplifier i. The notation is based on Miller and Zucker (1992).) In general we will choose the bounds α_i and β_i small and large enough so that they will not enter into the evolution of the system, so that we get the same form Hopfield (1984) gave for his equations:

$$\begin{aligned} c_i \frac{du_i}{dt} &= \sum_{j \neq i} T_{ij} V_j - u_i/R_i + I_i \\ V_i &= g(u_i) \end{aligned} \tag{2}$$

where $1/R_i = \sum_{j \neq i} T_{ij} + 1/\rho_i$. $|T_{ij}|$ is the conductance between the output of amplifier j and the input of amplifier i.[4]

As with our previous paper we do not assume the connections T_{ij} to be symmetric. However, consistent with the assumption stated in the introduction, we shall assume all $T_{ij} \geq 0$. For convenience but without loss of generality we will also assume $\alpha_{i,1} > 0$ for all i. This implies that the zero state, in which for all i, $u_i = 0$, is asymptotically stable (cf. Hirsch and Smale 1974) whenever the bias terms I_i are zero.

Let S be a nonempty set of amplifiers. Suppose there is an asymptotically stable unbiased equilibrium of (2) in which the amplifiers S have output 1, and all other amplifiers have output 0. We shall call such an S a *self-excitatory set*. Assuming nonsingularity of the system and nondegeneracy of solutions, we can make the following statement about S:

[4] In general we shall assume the scale of input to output is on the order of mvolts to volts (cf. Fig. 7, *bottom*), so that we can assume $R_i \approx \rho_i$, and hence the time constant of each cell is independent of the connection strengths.

Proposition 1. Let S be a self-excitatory set for the system (2), and suppose that for all amplifiers i, and u_i such that $\alpha_{i,1} \leq u_i \leq \beta_{i,\omega(i)}$

$$g_i(u_i) \geq \gamma_i u_i + \delta_i \tag{3}$$

where $\gamma_i = 1/(\beta_{i,\omega(i)} - \alpha_{i,1})$ and $\delta_i = -\alpha_{i,1}/(\beta_{i,\omega(i)} - \alpha_{i,1})$. Suppose a bias $I_i > \alpha_{i,1}/R_i$ is applied to each amplifier $i \in S$, and a zero bias is applied to all other amplifiers. Then the system will evolve from the zero state to an asymptotically stable state such that $V_i = 1$ for all $i \in S$, and $V_i = 0$ for all $i \notin S$.

Basically the proof shows how the system, viewed as a system of differential equations, can bring each neuron in the clique up to maximum potential, and that this state is stable. Eq. (3) is a single-slope version of the multi-slope Eq. (1) used to simplify the proof; the general case follows directly.

Proof. Assume first that

$$g_i(u_i) = \gamma_i u_i + \delta_i \tag{4}$$

for all i (cf. solid line in Fig. 7, *bottom*). The assumption that all T_{ij} are nonnegative implies that if the system is in a state at time t_0 such that $du_i/dt \geq 0$, for all i, then for all future times $t > t_0$ we have $du_i/dt \geq 0$, or in other words, all $u_i(t)$ are monotonically increasing. Furthermore, since all the amplifiers not in S start with zero output, and hence receive input only from members of S, they will, by the definition of S, continue to have zero output. After some finite time t, for each $i \in S$, the capacitor c_i will have charged, and we will have $\alpha_{i,1} < u_i \leq \beta_{i,\omega(i)}$. Because of the monotonicity of the $u_i(t)$, each u_i that reaches $\beta_{i,\omega(i)}$ will stay there. Therefore at time t, letting $\tilde{S}$ be the subset of S which have not already reached maximum output, (2) will be equivalent to a system of linear ordinary differential equations such that for all $i \in \tilde{S}$:

$$c_i \frac{du_i}{dt} = \sum_{j \in \tilde{S}-i} T_{ij}\gamma_j u_j - u_i/R_i + \left[I_i + \sum_{j \in \tilde{S}-i} T_{ij}\delta_j + \sum_{j \in S \setminus \tilde{S}} T_{ij} \right] \tag{5}$$

(The product with voltage = 1 term in the last sum is not shown explicitly.) With regard to the system (5) there are two possibilities: either it evolves to a point where $u_i \geq \beta_{i,\omega(i)}$, for some $i \in S \setminus \tilde{S}$, or it doesn't. In the latter case, by monotonicity of the $u_i(t)$, it must reach an asymptotically stable equilibrium $\hat{u}$ within the set $\prod_{i \in \tilde{S}}[\alpha_{i,1}, \beta_{i,\omega(i)})$. Let $T_{ii} = -1/R_i$ and assume the matrix $[T_{ij}]_{i,j \in \tilde{S}}$ defining (5) is nonsingular. Then the coordinatewise solutions $u_i(t)$ of (5) are, up to translation by the constant $\hat{u}_i$, linear combinations of functions of the form $t^k e^{ta} \cos(bt)$ and $t^l e^{ta} \sin(bt)$ where l and k are nonnegative integers and $a + bi$ is an eigenvalue of $[T_{ij}]_{i,j \in \tilde{S}}$. Assuming the nondegenerate case in which all eigenvalues affect each solution, we must have $a < 0$, or in other words, $\hat{u}$ is the unique asymptotically stable equilibrium of (5). Now consider (5) in the state $\overline{u}$ where $\overline{u}_i = \beta_{i,\omega(i)}$, for all $i \in \tilde{S}$. By the definition of S we know (5) can only evolve in a nondecreasing fashion from $\overline{u}$, and since $\hat{u}$ is the unique asymtoptically stable equilibrium for (5), $u_i(t)$ must actually increase with t for some i, and then decrease again as it moves toward $\overline{u}_i$. This is impossible since $u_i(t)$ is monotonic. We therefore have that for some $i \in \tilde{S}$, $u_i(t)$ reaches $\beta_{i,\omega(i)}$. Iterating the proof, we see that eventually $\tilde{S}$ will be empty and the proposition is proved for $g_i(u_i) = \gamma_i u_i + \delta_i$.

For the more general form (1) of g_i (cf. dashed line in Fig. 7, *bottom*) we simply observe that each $V_i(t)$ is bounded from below by the value of $g_i(u_i)$ given by (4) so that if, in the latter case, at some time $V_i = 1$, this will be true for the value of $g_i(u_i)$ given by (3). On the other hand, if for the case (4), $V_i(t) = 0$, for some i, this will continue to be the case for (3), since in both cases in the equilibrium state $u_i < \alpha_{i,1}$, and hence $g_i(u_i) = V_i = 0$. ■

For each amplifier i (not necessarily in S) let $S(i)$ be the set of all $j \in S$ such that $T_{ij} > 0$. Also let $T_{\max}$ ($T_{\min}$) be the maximum (minimum) over all T_{ij}. It follows that for each $i \in S$

$$c_i \frac{du_i}{dt} = \sum_{j \in S(i)} T_{ij} V_j - \beta_{i,\omega(i)}/R_i \geq 0 \tag{6}$$

hence

$$|S(i)|\, T_{\max} \geq \beta_{i,\omega(i)}/R_i$$

hence

$$|S(i)| \geq \left\lceil \beta_{i,\omega(i)}/T_{\max} R_i \right\rceil \equiv \xi_i^l \tag{7}$$

Conversely if

$$|S(i)| \geq \left\lceil \beta_{i,\omega(i)}/T_{\min} R_i \right\rceil \equiv \xi_i^u$$

then we must have $i \in S$.

Similarly, for each i $\notin S$ we must have

$$c_i \frac{du_i}{dt} = \sum_{j \in S(i)} T_{ij} V_j - \alpha_{i,1}/R_i \leq 0$$

hence

$$|S(i)| \leq \lfloor \alpha_{i,1}/T_{\min} R_i \rfloor \equiv \eta_i^u$$

and conversely if

$$|S(i)| \leq \lfloor \alpha_{i,1}/T_{\max} R_i \rfloor \equiv \eta_i^l \tag{8}$$

then we must have $i \notin S$. We state these results as a proposition:

Proposition 2. Let S be a self-excitatory set. Then $i \in S$ implies $|S(i)| \geq \xi_i^l$, and $|S(i)| \geq \xi_i^u$ implies $i \in S$. Also $i \notin S$ implies $|S(i)| \leq \eta_i^u$, and $|S(i)| \leq \eta_i^l$ implies $i \notin S$.

A self-excitatory set will be called *minimal* if no proper subset is also a self-excitatory set. For a simple example of a nonminimal self-excitatory set, note that the union of two distinct self-excitatory sets is necessarily contained in such a set. On the other hand, Proposition 2 immediately gives us an important class of minimal self-excitatory sets. This corresponds to the case where, in terms of its nonzero connectivity, S is a complete graph or *clique* on at least $\xi^u + 1$ amplifiers, such that for all $i \notin S$, $|S(i)| < \eta^l$, where ξ^u is the maximum over all ξ_i^u, and η^l is the minimum over all η_i^l. More generally we can let $S = \bigcap_{i=1}^k S^i$, where each set of amplifiers S^i is completely connected, and for certain of the pairs (S^i, S^j) such that $i, j \in \{1, \ldots, k\}$, $S^i \bigcap S^j$ is completely connected as well. The latter type of self-excitatory set could be distributed over a larger cortical surface than perfect cliques since it would not be necessary to connect the most distant cells corresponding to the most distant pairs (S^i, S^j). However we shall base our analysis for the remainder of this paper on pure cliques.

With respect to a clique of actual neurons it of course seems unlikely that a perfectly symmetric arrangement could arise in cortical development, and in fact the connectivity does not have to be perfectly symmetric for our analysis to hold. For example, with the clique sizes discussed in the next section, ten percent of connections could be randomly omitted with the primary negative effect on performance being to raise the self-sustaining activation level ξ_i^u by about that percentage.

3.2 Storage and Input Bounds for Random Data

Suppose we wish to store some collection C of randomly chosen self-excitatory cliques of amplifiers, each of size $M \geq \xi^u + 1$. The question we wish to address is how large we can reliably allow $|C|$ to be, and how many extraneous amplifiers we can allow to be biased in the process of retrieving a member of C. This amounts to evaluating the probabilities of two types of error events, following an attempt to activate a given clique $C^p \in C$ by biasing a set of amplifiers E sufficient to saturate C^p. While E will of course not be independent of C^p, we shall assume that $E \setminus C^p$ is independent of the other $C^q \in C - C^p$. Also we shall assume that formation of a clique that connects amplifiers j to i does not change the value of an existing connection $T_{ij} > 0$.

Error type 1 occurs when there exists an amplifier $i \notin C^p$ with an input bias from C^p that causes it to have a significant nonzero output. A necessary condition is thus

$$\sum_{j \in C^p} T_{ij} V_j > \alpha_{i,1}/R_i$$

However observe that for a response curve such as the dashed line in Fig. 7, *bottom*, with a large initial slope, requiring

$$\sum_{j \in C^p} T_{ij} V_j \leq \alpha_{i,1}/R_i$$

is unnecessarily stringent, since the response has the same nonsaturated level for a bias considerably larger than $\alpha_{p,1}/R_p$. In terms of the *top* and *middle* graphs of Fig. 7, we get just a single spike in a 25 msec time interval for any bias between .3 and .6 nA. Thus the level of bias which we shall view as a type 1 error can be more reasonably taken as

$$\sum_{j \in C^p} T_{ij} V_j \geq \beta_{i,\omega(i)}/2R_i \tag{9}$$

Similarly to (8) we define

$$\eta_i \equiv \left\lceil \beta_{i,\omega(i)}/2T_{\max}R_i \right\rceil \tag{10}$$

which is the least number of nonzero connections that could cause amplifier i to have an input $\geq \beta_{i,\omega(i)}/2$, and let η be the minimum over all η_i.

Error type 2 occurs when at least one of the cliques $C^q \in C - C^p$ can be saturated by $E \bigcup C^p$.

Observe that errors type 1 and 2 produce unwanted effects that persist after the bias E which saturates C^p is removed. It is only these persistent effects that we shall be interested in, since the state of the system during the biasing by E is not otherwise relevant to the final computation.

Of course the connections that form the cliques in C can inadvertently form new self-excitatory sets, either by extending members of C or creating entirely new self-excitatory sets that contain no member of C as a subset. However we shall arrange for the expected number of type 1 errors to be sufficiently small, so that the probable number of amplifiers involved in either of these scenarios will be small, and thus may be neglected. Thus we shall assume that with C^p saturated, the only remaining self-excitatory sets that $E \setminus C^p$ could activate are those in C.

To estimate the probability of a type 1 error, note that, with respect to (9), this event can only occur if i and at least η^l such j are in the same clique. That i and any other random amplifier j are in the same clique has probability

$$\rho = 1 - \left(1 - \frac{M}{N}\frac{(M-1)}{(N-1)}\right)^{|C|-1} \tag{11}$$

If M is small relative to $|C|$, the probability of obtaining at least $\hat{\eta}$ such matches for $j \in C^p$ will be given approximately by the binomial distribution, that is

$$\sum_{k=\eta}^{M} C(M,k)\rho^k(1-\rho)^{M-k} \tag{12}$$

Let X_i be the indicator (0 or 1) random variable for amplifier $i \notin C^p$ receiving the input (9) from C^p, and let $E()$ denote expectation. Then since expectations add the total expected number of such amplifiers is

$$E\left(\sum_{i \notin C^p} X_i\right) = \sum_{i \notin C^p} E(X_i) = \sum_{i \notin C^p} \mathrm{Prob}\{X_i = 1\} \tag{13}$$

Thus since $\mathrm{Prob}\{X_i = 1\}$ is approximately (12), requiring (13) to be $\leq \epsilon$ is approximately equivalent to

$$(N-M)\sum_{k=\eta}^{M} C(M,k)\rho^k(1-\rho)^{M-k} \leq \epsilon \tag{14}$$

which, solving as an equality for ρ, gives us an upper bound $\rho_\epsilon \leq \rho$. Alternatively we can use the Poisson approximation

$$(N-M)\left(1-e^{-\rho M}\sum_{k=0}^{\eta-1}\frac{(\rho M)^k}{k!}\right) \leq \epsilon$$

From (11) we observe

$$|C| \leq \frac{\ln(1-\rho_\epsilon)}{\ln\left(1-\frac{M(M-1)}{N(N-1)}\right)}+1$$

where ρ_ϵ is the solution to (14).

If we choose ϵ sufficiently small, say ≤ 1 (cf. Willshaw et al.,1969, p. 961), the binomial distribution with a large number of trials and small success probability per trial becomes a reasonable approximation, and we may in turn approximate the latter with the Poisson distribution, so that the probability of k type 1 events is $\exp(-\epsilon)\epsilon^k/k!$ and in particular the probability of no type 1 events is $\exp(-\epsilon)$.

Now let us consider the probability of a type 2 error, assuming $\epsilon \leq 1$ as above. Since the probable number of type 1 errors is being kept small, we shall neglect them, and simply assume, using as an upper bound the binomial distribution in (12), that each of the $N-M$ amplifiers outside C^p receives a bias from C^p and the other biased amplifiers E which is

$$\leq T_{\max}\left(\rho_\epsilon(M+|E|/2)\right) \equiv \hat{I}$$

Adding the bias $\hat{I}$ to the left-hand-side of (6) we derive a new version of (7), namely

$$|S(i)| \geq \left\lceil\left(\frac{\beta_{i,\omega(i)}}{R_i}-\hat{I}\right)/T_{\max}\right\rceil = \left\lceil\frac{\beta_{i,\omega(i)}}{T_{\max}R_i}-\rho_\epsilon(M+|E|/2)\right\rceil \equiv \xi_i$$

or in other words, neglecting ceilings,

$$\xi_i = \xi_i^l - \rho_\epsilon(M+|E|/2)$$

Let ξ be the minimum over all ξ_i. Then the probability of a type 2 error for arbitrary $C^q \in C - C^p$, using the hypergeometric distribution, is

$$\leq \sum_{k=\xi}^{M}\frac{C(|E|+M,k)C(N-|E|-M,M-k)}{C(N,M)}$$

Thus if $\hat{\epsilon}$ is a desired bound on the probability of a type 2 error, we can set

$$1-\left[1-\sum_{k=\xi}^{M}\frac{C(|E|+M,k)C(N-|E|-M,M-k)}{C(N,M)}\right]^{|C|-1} = \hat{\epsilon} \tag{15}$$

and solve numerically for $|E|$.

As opposed to ϵ, which was an expected value which we could plausibly leave at about 1, $\hat{\epsilon}$ is a probability which should be small, since setting off the wrong clique ruins the computation. Exactly how small $\hat{\epsilon}$ should be would depend on how sensitive higher level mechanisms would be to an error. Biologically one would expect some tolerance, so we will take $\hat{\epsilon}$ as 10^{-4}. In fact the specific choice of $\hat{\epsilon}$ is not very critical, since the probability of a type 2 error goes effectively from zero to one within a relatively narrow range of $|E|$.

In order to give some computed examples, we need to specify or provide ranges for the additional parameters. We shall assume in all our examples that the T_{ij} are independently distributed around a mean T_μ such that $(M/2)T_\mu = \beta_{i,\omega(i)}/R_i$ for all i, with standard deviation $\sigma = T_\mu/2$. Thus biasing above threshold $M/2$ members of a clique, all of whose members have connections T_μ, will be just sufficient to activate the clique. Since the average output of n random amplifiers will then be T_μ with standard deviation $\sigma/\sqrt{n}$, we can, in order to get a reasonably tight lower bound on the maximum values of $|C|$ and $|E|$, take $T_{\max}$ as $T_\mu + \sigma/\sqrt{n}$. Then substituting in (7) gives us

$$\beta_{i,\omega(i)}/\left[R_i\left(\frac{\beta_{i,\omega(i)}}{R_i}\frac{2}{M}+\frac{\beta_{i,\omega(i)}}{R_i}\frac{1}{M}/\sqrt{\xi_i^l}\right)\right]=\xi_i^l$$

which solving as a quadratic (in $\sqrt{\xi_i^l}$) gives us

$$\sqrt{\xi_i^l}=\frac{-1+\sqrt{1+8M}}{4}\Rightarrow \xi_i^l\approx\frac{M}{2}$$

Similarly from (10) we have

$$\sqrt{\eta_i}=\frac{-1+\sqrt{1+4M}}{4}\Rightarrow \eta_i\approx\frac{M}{4}$$

With regard to the size of N, we provide a range of 10k to 400k.

Note that each clique takes M^2 connections, and with our choice of ϵ each connection will generally belong to just one clique, so we must have $M^2|C| \leq Nf$, where f is the average dendritic fan-in, and hence

$$|C| \leq Nf/M^2 \tag{16}$$

Taking the dendritic fan-in for a pyramidal cortical cell of 6,000 (Douglas and Martin 1990) as a value for f, we obtain the graphs for $|C|$ and $|E|$ in Fig. 8, *top* and *bottom*, respectively.

4 Application: Hyperacuity-scale Representations of Lines in the Visual Cortex

We now proceed to show, using the cortical model described in the previous sections, that groups of pyramidal cells in human and monkey primary visual cortex are capable of representing short line contours on hyperacuity scales. By "hyperacuity" we mean specifically the ability, under optimal circumstances, to discriminate straight line contour orientations an order of magnitude better than our ability to resolve two stars (or other points of light), when we are comparing the displacement of the endpoints of the contour with the separation of the stars (Fig. 6). [5] For the sake of this analysis, we assume that pyramidal cell counts in monkey and human visual cortex are comparable.

To carry out this analysis we view each line contour as an item of information in a database consisting of subsets of cortical neurons. Hyperacuity can then be interpreted as the ability to store a certain amount of information in this database corresponding to an extremely large number of such subsets. The question then becomes whether the brain is equipped to do this. Our answer is in the affirmative, under the assumption that excitatory cliques of S cells exist, and leads to the surprising result that cliques are smaller than one might expect on intuitive grounds. In the end we argue that cliques should consist of about 33 cells.

4.1 On the Existence of Excitatory Cliques Of S Cells

We begin by expanding on points raised in the introduction. The connectivity described by Rockland and Lund (1982) and Rockland et al. (1982) in tree shrews, Rockland and Lund (1983) in monkeys, and by Gilbert and Wiesel (1983, 1989) and Callaway and Katz (1990) in cats, seems ideal for connecting groups of cells which respond to approximately the same contour orientation. The result is a visual field significantly greater than the individual receptive fields. We illustrate this in Fig. 1, which shows a thin moving slit of light and three rectangular receptive fields (cf. Fig. 4 *bottom*) whose corresponding cells each simultaneously respond to one edge of the slit (cf. Fig. 4 *middle*, and Fig. 4 *bottom*). Thus the connectivity requirement would seem to be met.

Within this connected clique, how do we know that such a group of S cells can respond, as a group, to a specific contour? In particular, how do we know, first, that it is S cells (Henry 1977, Bishop et al 1971, 1973, 1972, Hubel and Wiesel 1962) which are being interconnected, and secondly, how do we know that these cells are responding in a precise spatio-temporal fashion to *moving* stimulus contours?

With regard to the first question we must consider both substantive and (for historical reasons) nomenclature issues. Both Henry et al. (1979, Fig. 2A) and Martin (1984, Fig. 13) have found that the majority of identifiable superficial layer cells in cats are either type-S, or type-S endstopped (S_H). Again, while it is tempting to identify S cells (Henry 1977) with simple cells (Hubel and Wiesel 1962), one must be careful (cf. Gilbert and Wiesel 1979, Martin 1984); we stress that our focus on S cell types, rather than on the "simple" cell type, is the spatio-temporal aspect of the definition. Schiller et al. (1976a) have found a substantial proportion of the identifiable cells in superficial macaque layers to be of this type (which he also calls "S"), as well as of another larger type which he identifies as "CX". However they observe that these superficial layer CX cells have the receptive field size, orientation tuning, endstopping, binocularity, and low spontaneous spiking more typical of their "S" cells. A major reason for not putting these cells in the S category is the inability to distinguish a

[5] A prior conjecture has been put forth by Barlow (1979) that the basis for hyperacuity lies in sufficiently large populations of granule cells in primary visual cortex. However he did not propose a network model, and based on the network model described here, granule cells seem much less likely candidates than pyramidal cells, due to their shorter range and lower degree connectivity.

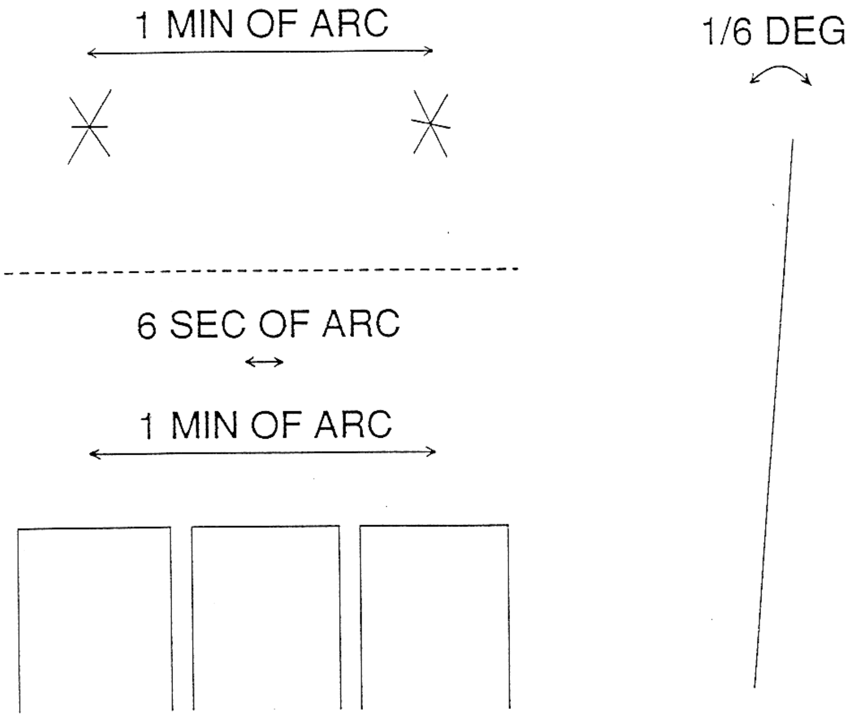

Figure 6: Comparison of normal acuity and hyperacuity. (*Upper Left*) Two point light sources such as stars separated by 1 min of arc correspond at the human fovea (*lower left*) to a separation of the two peak image intensities of two cone spacings. Thus both theoretically and empirically 1 min of arc is the smallest resolution of two points of light. However, for a thin line contour .5 deg in length as in (*right*), we can detect a change in orientation of as little as 1/6 deg, representing a relative displacement in the endpoints of only 6 sec of arc, or 1/5 of an average cone separation (cone represented as rectangle) (*lower left*) and thus far exceeding normal resolution limits. This is an example of *hyperacuity*. (Adapted from Westheimer 1990.)

relatively large spatial separation between the cell's edge-response regions. From our point of view such a criterion is very significant and if this were the only difference we would call these S cells. We note Schiller et al. 1976a, Fig. 13 as an example of this type of cell, which, if one were using the separation criteria described in Fig. 3 instead of Gaussian fitting, could have been classified as an S cell. Thus S cells appear to exist in layer 2/3; many of differences in the literature may be largely nomenclature.

As for the second question, we know that hyperacuity phenomena occur in the presence of significant motion of 3 deg/sec or more, and indeed some degree of motion can actually *improve* hyperacuity (Westheimer and McKee 1975). Given this tolerance to motion, the precise spatial and temporal response acuity cited above to moving edge contours would appear to be a basis for a highly specific group response to these stimuli, provided one could count on a certain continual contour motion. This is certainly the situation, at least for humans, whose eyes experience ongoing motions due to tremor, drifts, and micro-saccades (Alpern 1962).

Given that a highly interconnected group or *clique* of S-type pyramidal cells can exist and can respond as a group to a highly specific stimulus contour, what is the dynamic behavior of this group that makes its presence known to the rest of the brain, and which distinguishes it from mere noise?

First we recall that such cells typically exhibit the adaptive spike train behavior in Fig. 3 and further note that the early interspike intervals tend to vary systematically and dramatically with the input current (Fig. 7, *top*). From the point of view of each member of a clique, that cell's own behavior is determined, not by its own sparse intermittent spiking, but by the output of the rest of the clique. To enable calculation, and for reasons that will become clear shortly, suppose there are 33 cells/clique. Now, if we assume simultaneous first spikes followed by Poisson interarrivals for the second spike, would produce the incoming spike rate for each cell in the first 3.5 msec as given in Fig. 7, *middle*. This kind of input/output relation, with its relatively high and randomized *group* spike rate and short time interval in relation to each neuron's time constant of 10-20 msec (Douglas and Martin 1990) permits, first, an analog approximation to the input current, and second, the assumption of an approximately linear current-voltage relationship for each cell. We therefore can model each cell with a purely analog, piecewise-linear input/output voltage amplifier as in Fig. 7, *bottom*.

We have discussed such piecewise-linear amplifiers in a previous paper (Miller and Zucker 1992), where we showed that they have certain computationally attractive properties for modeling nonsymmetric analog recurrent networks. We show in a separate paper (Miller and Zucker 1998) that these results imply that the cliques we are interested in can be modeled and computed in a manner that scales-up efficiently with the size of the network. The main point here, however, is that excitatory cliques of such amplifiers tend to exhibit a dynamic behavior which drives each member of the group to saturation response. Given that cells in primary visual cortex are normally quiescent, we can assume that a substantial number of cells in superficial layers responding within a single 25 msec interval at saturation levels would be a sufficiently unlikely event to reliably identify this group of cells as an excitatory clique responding to a specific class of visual input.

It is important in this model of self-excitatory neuronal cliques that each clique member,

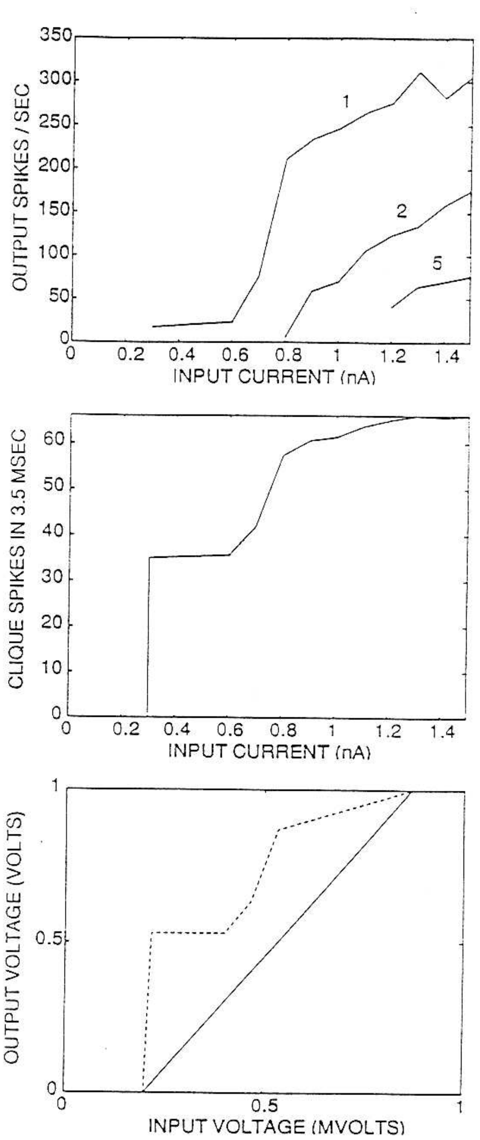

Figure 7: Comparison of cortical pyramidal cell input/output with that of model neurons. (*Top*) First, second, and fifth interspike intervals in spikes/sec as a function of input current for a rat layer 5 pyramidal cell (redrawn from Douglas and Martin 1990). (*Middle*) Expected total spike output during 3.5 msec of a hypothetical clique of 33 neurons of the kind described in *top*, interpreting the spike rate of each of these neurons as the arrival rate of an independent Poisson process. Each member of the clique experiences the clique output as input, so that we may model the clique response as a whole with an equivalent collection of purely analog amplifiers as in *bottom*. (*Bottom*) Since a cortical somatic time constant is typically much larger than 3.5 msec (e.g. 10-20 msec [Douglas and Martin 1991]), we may assume an approximately linear current-voltage relation, and thus model a clique of these cells with a clique of voltage amplifiers with the same shape input/output function. Examples of possible input/output function for piecewise-linear voltage amplifiers used in model neurons. Simplest is given by solid line. A more complicated function based on that empirically derived in Fig. 7, *middle*, is given by dashed line.

under a typical lower level afferent stimulation be capable of responding with at most one or perhaps two spikes within a temporal precision of a few msec. The occurrence of such spikes in a large enough percentage of a given clique's neurons constitutes in our theory the match that ignites the entire clique to saturation firing. However the brain must be able to distinguish the match from the conflagration. Thus it is important that lower level afferent stimulation produce a typical spike train which is *not* characteristic of saturation firing. Notice that in Fig. 7, *top*, we can describe the single spike response (within a given 25 msec interval) as corresponding approximately to an input current of $\leq .7$ nA, whereas saturation response is reached at about twice that input level. Thus this kind of cell appears to have a dynamic range of response which is perfectly suitable for distinguishing between single spike and saturation response. Furthermore we note that a typical one or two spike response of layer 3 pyramidal cells to LGN afferents has been observed both empirically and with compartmental models (Douglas and Martin 1992); see Konig and Engel (1995) for a more general review of relevant data.

4.2 An Analog Random Storage Model: Storage Capacity and Resistance to Noise

We now consider the question of whether enough self-excitatory cliques in the primary visual cortex can be stored to represent lines on hyperacuity scales. Additionally we can determine how resistant the resulting system would be to noise.

We begin by considering an idealized model in which cliques of a specified size M are chosen at random from the total population of neurons and then completely interconnected. The interconnection (i.e. synaptic) strengths are themselves independently distributed around a mean T_μ such that $M/2$ members of this clique at full output would be just sufficient to maintain another member of the clique at full output, given that the connection strengths to this other member were all T_μ. The standard deviation of the connection strength is chosen to be half the mean value.

Fig. 8, *top*, gives lower bounds, calculated in Section 3.2, on the number of storable randomly chosen cliques for four clique sizes M, as a function of the neuron population N. These bounds are designed to insure that the expected number of model neurons inadvertently saturated by an activated clique is ≤ 1. Observe that eventually curves for all values of M become the linear function Nf/M^2, as all f available synapses per cell are used up (we assume $f = 6000$ for pyramidal cells [Douglas and Martin 1990]). Thus the curve for $M = 60$ reaches its linear bound at a much lower value ($N \approx 100$k) than the curve for $M = 25$ ($N \approx 350$k). On the other hand the curve for $M = 15$ does not even come near its linear bound on this graph, owing to the necessarily high level of excitability of a system of very small cliques which can maintain themselves at saturation response. Observe also that even for $M = 25$, which was about the maximum in terms of ratio of cliques to neuronal population over the range considered ($N \leq 400$k) the linear bound is reached at about $N = 350$k, which corresponds to an area of primary visual cortex of about 3 mm^2 in monkeys, and about twice that in cats and rats (Peters 1987). At this point this ratio is about 9.6 for $M = 25$. Similarly for $M = 33$ the maximum ratio is reached at about $N = 290$k, and has a value of about 5.5.

In Fig. 8, *bottom*, we consider, for the same model and clique sizes given in Fig. 8, *top*, lower bounds on the number of randomly chosen additional model neurons which could be given an impulse current sufficient to produce a single spike (corresponding to lower level afferent input), without inadvertently setting off a clique in addition to the one targeted. More specifically we wish to keep the probability very low for such an event. Details of the calculations were given in Section 3.2. We can view these additional randomly activated model neurons as noise, and therefore the number of such model neurons which are allowable as the system's tolerance to noise. Observe that, for example with $M = 33$, the noise tolerance is in general at least twenty times greater than the clique size.

4.3 Mapping from a Region of Visual Field to a Region of Cortex

We suppose now that the brain is trying to store in a $(6 \text{ mm})^2$ region A^c of primary visual cortex local information about line contours within a visual field A^{vf}. Portions of these regions are illustrated in Figs. 3 and 6, respectively. Assuming a human foveal magnification of 15 mm/deg, there will be a mean shift in receptive field location of the cells of A^c by about 24 arc minutes, traversing its width. The receptive fields for cells in A^c will however have a mean width of about 12 arc minutes (Wilson et al., Fig. 9) so that we may take A^{vf} to be approximately $(36 \text{ arc minutes})^2$. In fact A^{vf} could be taken as somewhat larger due to a radial scatter of about half the receptive field size in either direction (cf. Albus 1975, Hubel and Wiesel 1977), but this would result in a rapid drop-off in density of receptive field coverage of A^{vf} toward the borders.

Note that A^c will include about the widths of four human orientation columns, assuming human iso-orientation patterns are similar to the macaque (e.g. Ts'o et al. 1990) and using the scaling factors for human ocular dominance columns (Horton et al. 1990). Thus we may assume that the receptive fields of the S-type cells in A^c have uniformly distributed orientations in A^{vf}. Note however that the receptive field centers, although radially symmetric, will be somewhat more concentrated towards the center due to the above-mentioned radial scatter.

4.4 Calculation of Cortical Packing Density from Hyperacuity Data

We shall now calculate both the clique size M and the cortical packing density of S-type pyramidal cells necessary for a sufficient number of cliques to perform hyperacuity-scale discriminations of straight line orientations. We shall assume that all available synapses are being efficiently utilized in the formation of cliques, which would correspond in the above random storage model to the assumption that the appropriate curve in Fig. 8, *top*, has reached its linear bound of Nf/M^2. Otherwise all parameter assumptions are based on empirical observation.

We assume the network of S-type cells is storing the cliques efficiently, that is, near its capacity of $|C|$ cliques, each of size M, where C is the total set of cliques. Then each S cell must, on average, belong to

$$|C|M/N$$

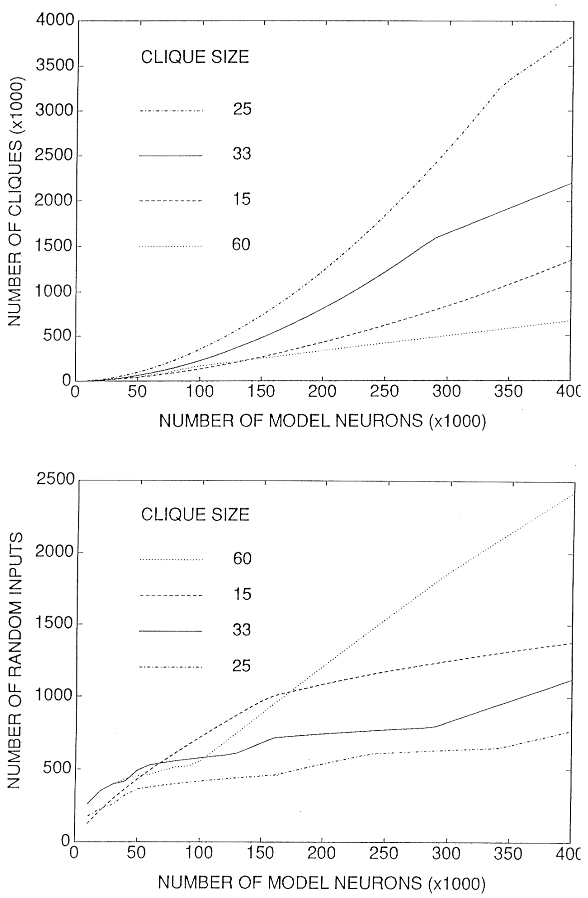

Figure 8: Number of cliques and noisy inputs as a function of network size. (*Top*) Computed lower bounds on the maximum numbers of randomly chosen self-excitatory cliques which can be formed in a network of analog model neurons as described in text, as a function of number of neurons N, for clique sizes 15, 25, 33, and 60. Note in all cases, except size 15, for sufficiently large networks the number of cliques becomes limited by the number of connections available, so that the graphs become linear in N, taking the value Nf/M^2, where f is the dendritic fan-in and M is the clique size. (*Bottom*) Maximum number of random inputs (noise) in addition to coherent input for same clique sizes as above, and assuming the number of cliques stored is at the maximum as given above. (See text, Section 3.2, for calculation of top and bottom graphs.)

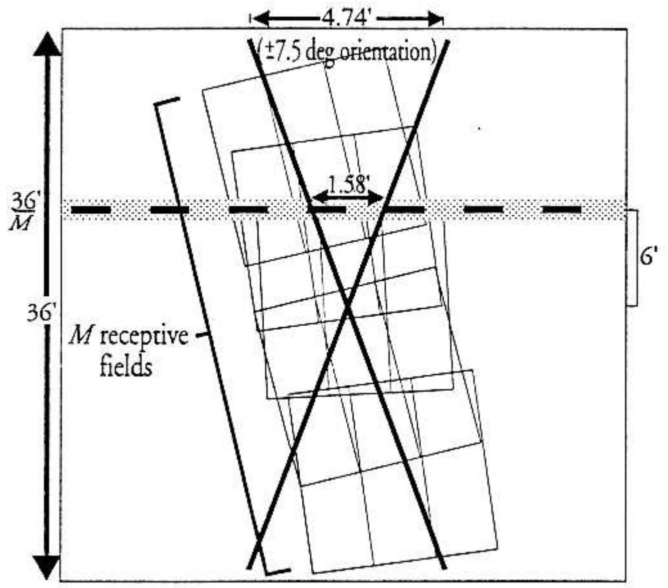

Figure 9: Orientation hyperacuity and cortical cell density. A model S cell with an orientation tuning width of 15 deg, whose receptive field is at the center of the visual field represented here, belongs for each edge-response location (vertical lines within rectangular receptive field) to 90 cliques of cells representing 90 line orientations, based on orientation hyperacuity of 1/6 deg (see text for calculation). Each line clique consists of M receptive fields (shown here for one orientation). The angle has been exaggerated for display purposes.

cliques. (To consider a totally *inefficient* arrangement imagine each cell belonging to just one clique, so that the number of cliques is $N/M \ll |C|$.)

Now let us consider an S cell which belongs primarily to straight line cliques of the kind indicated in Fig. 1.

We assume (Bishop et al. 1971, 1972, 1973; Schiller et al. 1976 a,b,c) that an S cell responds to a slit of light or a bar by responding to its edges. In general this response is direction dependent, and may strongly depend on variable and relatively nonspecific inhibition (Bishop et al. 1973). For this analysis we shall make the simplifying assumption that each cell responds to both light and dark edges, but only in one direction. [6] Thus the distinctly shaded regions in each receptive field in Fig. 1 are not to be taken as separate ON/OFF regions, but rather their borders are to be taken as the points on the axis perpendicular to orientation of maximum probability of initial spike response to a particular edge, in a particular direction of motion.

For the network to be efficient there must be $|C|M/N$ distinct contours passing through its receptive field, skirting either of its side regions.

From geometry it is clear that the only way this can happen is for the contours to have varying orientations. In fact for each orientation there are just two contour positions that would put the cell at the appropriate place on its response tuning curve, one corresponding to each inhibitory flank.

We therefore shall assume that each S cell belongs to exactly two cliques for each discriminable orientation of a contour within its tuning range, which in monkeys will be about 15 deg before a steep falloff of over ten percent in average response occurs (Hubel and Wiesel 1968; De Valois et al. 1982, Fig. 1C; Schiller et al. 1976b, Fig. 2). If h is the number of cliques (hence lines) per degree, this means

$$|C|M/N = 2 \times 15 \text{ deg} \times h \tag{17}$$

We assume that storage is at its limiting value of

$$|C| = Nf/M^2 \tag{18}$$

Martin (1984) has found that S cells in cats may be both layer 2/3 pyramidal and spiny stellate, so it is not clear a priori whether to take these cells' respective fan-in values f of 2000 or 6000 (Douglas and Martin 1990). However since it is between layer 2/3 pyramidal cells that the intrinsic horizontal inter-iso-orientation area connections have been observed by Gilbert and Wiesel (1983, 1989) and Callaway and Katz (1990), it is the pyramidal fan-in figure of $f = 6000$ which appears most justified. Furthermore the data from orientation hyperacuity (Westheimer 1990) implies a value of h in (17) of 6 lines/deg. Therefore (17) and (18) imply

$$h = \frac{(Nf/M^2)(M/N)}{2 \times 15 \text{ deg}} = 6 \text{ lines/deg}$$

[6] This was the most common class of S cells found by both Bishop et al. (1971) and Schiller et al. (1976a).

which implies

$$M \approx 33$$

Observe this clique size is about optimal for the random model if we give equal weight to both clique capacity and noise tolerance (Fig. 8, *top* and *bottom*). This also supports the assumption made in Sec. 4.1 about clique size.

What about the size of N? Let us look at the S cell population from the point of view of a single S cell whose receptive field is centered in A^{vf} and oriented vertically (Fig. 9). There are $15 \times 6 = 90$ contours passing through a given side of its receptive field. Although there may be some overlap between the corresponding orientation cliques of any two of these, N must be chosen so as to keep such an overlap to less than half. Thus if we consider the 1.58 arc minute window, 6 arc minutes above the center line, through which all these contours have to pass, and which is 36/33 arc minutes deep (Fig. 10), there must be, on average, at least 90 distinct appropriately oriented S cell receptive fields to accommodate them. Here we assume that 6 arc minutes above center represents a mean horizontal receptive field density, and that $M = 33$ as derived above. This gives us a receptive field density of

$$90/(1.58 \text{ arc min} \times 36/33 \text{ arc min}) = 52.2/(\text{arc min})^2$$

Allowing for the 12 other orientation ranges to accommodate 180 deg, we get 626.4 receptive fields per $(\text{arc min})^2$ or 812k for all of A^{vf}. Translating this back to A^c gives us a minimum sufficient density of 22.6k S cells per mm^2 of foveal cortex. Allowing for enough cells to accommodate the opposite direction of motion as well, we would need to double the cell count to 45.2k cells per mm^2.

In comparison we note that the number of layer 2/3 pyramidal cells that have been estimated for macaque monkey primary visual cortex (Peters and Sethares 1991, Fig. 19 and Table 1, and assuming 10 percent GABAergic cells), is

$$(35\text{cells/cluster}) \times (1271\text{clusters/mm}^2) \approx 44.5\text{k cells/mm}^2$$

5 Discussion

We have presented a model of cortical computation which is sophisticated enough to model a range of biological events in the visual cortex, but simple enough to be subject to mathematical analysis. In any such undertaking there will invariably be modeling simplifications that have important consequences, and parameters whose specification can not be determined more than approximately by existing objective measurements. Several of these exist here. In particular, because of the focus on orientation hyperacuity at a point, we did not consider the question of nearby cliques in the direction orthogonal to the bar orientation. The analysis concentrated on the orientation variability and the effects of length; it remains to be seen whether this additional analysis will keep the cell counts consistent. Regarding parameters, the chosen area A^{vf}, the 6 arc minutes vertical displacement chosen in Figs. 9 and 10, the assumption that each S cell responds to exactly two edges, and the length of the

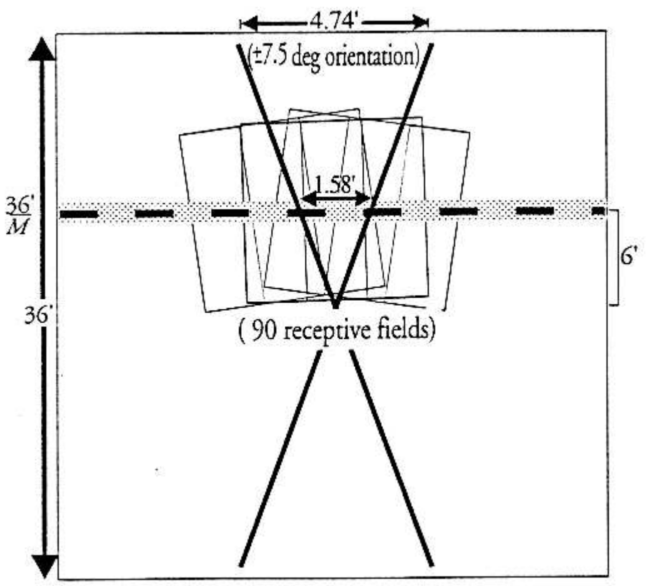

Figure 10: Completion of density calculation begun in Fig. 9. In order for the line cliques to have enough cells to fill them without excessive overlap between any two cliques, there must be about 90 receptive fields whose centers are within the region $36/M$ arc min high (shaded) by 1.58 arc min wide (between labeled arrows), and which is located about 6 arc min above center (dashed line). From these numbers we can calculate an overall cortical density for this kind of cell (see text).

contour to which the cliques are responding could of course have been chosen somewhat differently. Somewhat different results would then have ensued. However, we have attempted to choose parameters that seem representative, given the existing empirical data and species differences. What is remarkable about the outcome of this procedure is that a prediction of monkey cortical cell packing densities could be derived for any reasonable choice of parameters which agreed to within an order of magnitude or two. Our result of 45.2k predicted vs 44.5k observed should clearly be taken as a first example calculation; no doubt more complete models and more careful estimates will be possible in the future. Nevertheless, we believe it provides an argument in support of the class of clique-based computations proposed.

Our model addresses the question of how information can be represented in the brain in a way that is consistent with known anatomical, physiological, and biophysical facts. Our model provides a clear description of how the brain could go about representing great masses of information – in this case pertaining to the orientation of lines and visual hyperacuity – in a way that at the same time implies a high degree of reliability from inherently unreliable units, i.e. neurons. Additionally our model says how this can be done in a time scale, 25 msec, which we know is necessary in order to make lower level processing available sufficiently quickly to the rest of the visual system. None of these features is addressed by a theory based on a vector averaging of long-term cortical cell responses.

Furthermore, our model makes the testable prediction that there exist cliques of layer 2/3 pyramidal cells in human, monkey, tree shrew, and cat primary visual cortex which are close to being completely interconnected synaptically, and which can drive themselves to saturation feedback responses within periods of approximately 25 msec in response to small lines or edges moving in a specific direction perpendicular to orientation. Furthermore the model predicts that in monkeys and humans the number of such cliques is several times larger than the actual population of cells from which they are formed, and that the average size of these cliques is about 33.

Let us consider the reliability issue further. There are intimate connections between the present work and traditional reliability theory (cf. Winograd and Cowan 1963). Roughly speaking we are suggesting that line detection on hyperacuity levels consists of activating a K-out-of-M or *quorum* component system (Moore and Shannon 1956). In this context, we can view each neuron as a component, and each clique as a system. As the appropriate contour (or a corrupted version) passes through the visual field, a neuron has a certain probability $p > .5 + \epsilon$ of spiking at least once, whereas in the absence of such stimulation the neuron's probability of spiking is $p < .5 - \epsilon$. In Fig. 5 we give the probability for a 17-out-of-33 clique to respond as a function of its component neurons' probabilities of firing. In effect, the clique transforms a group of highly unreliable response units (small ϵ) into a single reliable system.

The 17-out-of-33 system above is of course just one possible example of a K-out-of-M clique, although we have described in the Section 4 our reasons for choosing $M = 33$. Our theory does not however imply a specific value for K, and indeed, in deriving the lower bounds on number of cliques and tolerance to noise in Fig. 8, we have assumed that K is at least $M/2$, although smaller values are possible. Obviously however K must be substantially less than M if the system is to improve the reliability of individual cortical neurons. In any event the model implies that the number of EPSP's from superficial layer pyramidal cells needed to produce an action potential in another such cell is less than about 33, and probably closer to 17. These numbers are low compared to what is necessary, for example, to elicit action potentials in spiny cells in the hippocampus (McNaughton et al. 1981), but are consistent with estimates for activation of layer 4 S cells being directly innervated by the LGN (Bullier et al. 1982), given that each LGN afferent in general forms only one synapse for each target cell (Freund et al. 1985).

The degree of lateral precision implied by orientation hyperacuity (cf. Figs. 9 and 10) is sufficient to account for both standard vernier acuity, and the 2-dot variety demonstrated by Westheimer and McKee (1977). Interestingly, the 2-dot phenomenon, as Westheimer and McKee remark, could also be explained by an orientation model capable of detecting incomplete or implicit lines, which our model is capable of doing. In terms of orientation discrimination, the optimal separations for outsides of the 2-dots were about 6 arc min, and for the endpoints of the complete lines were about 6 arc min or higher (Westheimer 1982, Fig. 1). It is therefore interesting to note that our model, together with the receptive field layouts illustrated in Figs. 9 and 10, implies that, as the length of the contour is reduced and its endpoints brought closer together, the maximum number of distinct cliques whose receptive fields would be approximately centered at these endpoints is also proportionately reduced. This in turn implies that the maximum line orientation discrimination ability (in degrees of rotation) is proportionately reduced (since angles are small), given that the lateral discrimination of the endpoints remains constant. Our model predicts that these relations should hold down to a point determined by the edge-response characteristics of the receptive field, at which performance deteriorates. This in fact seems consistent with what has been observed (Westheimer 1982, Fig. 1, *bottom*; Westheimer 1990).

We have remarked in the preceding section that we do not expect the visual cortex to be able to form perfectly interconnected cliques, nor is it clear that this would even be desirable from an efficiency viewpoint. As we have remarked in the previous section, many kinds of incompletely connected self-excitatory groups of neurons could exist which would span considerably larger areas of cortex than a totally connected clique could, and we have described a general class of these. Furthermore a significant percentage of connections from any clique could be randomly removed with the only possibly negative effect being to increase the number of spikes needed for activation of the clique. The implications for learning (e.g., Löwel and Singer, 1992) and for fast synaptic facilitation deriving from this model should also be mentioned (Varela et al, 1997; Fischer et al, 1997).

There are several related issues that we have not addressed in this paper, perhaps the most important of which involve the relationship between spatial vision and motion. All of the constructs were based on slowly moving visual stimuli of the type that are natural for S-cells. One way to take this model into the motion domain is to postulate a sequence of cliques at nearby positions that fire in temporal sequence. This seems natural for slowly-moving configurations, in which the additive inhibition or each cell's biophysics would bring each clique down to quiescent, and an adjacent clique would ignite. To place some rough numbers on this, we might calculate that (according to the data in Fig. 4 and the model in Fig. 7), the stimulus moves about 3 min. in the time it takes for the clique to saturate. Now, from the Westheimer (1990) constraint of 6 lines/degree, we calculate that there is about a factor of 4 before the next clique must saturate, which should be sufficent. However, what this implies for apparent motion must be checked and whether cells with different "velocity labels" exist must be considered. Moreover, this model at high stimulus velocities is questionable, and perhaps other velocity-encoding techniques should be considered.

In its most general terms, our theory suggests the necessity for a precise distinction between the *individual* response of a cortical neuron to lower level afferent stimuli and that neuron's response *as part of a cortical group.* To observe cortical cliques as functioning entities would require disentangling the two types of cell firings. Important steps in this direction have already been taken by a number of the works which we have cited, and we believe this trend should be accelerated. The rewards could be a very considerably increased understanding of the visual cortex, and perhaps other parts of the brain as well.

6 Acknowledgments

We thank Gerald Westheimer, David Jones, and Allan Dobbins for valuable discussion, David Tank for (repeatedly) stressing dynamics, and Rodney Douglas for kindly supplying the data used in Fig. 3. The reviewers were extremely helpful.

Research supported by grants from AFOSR, NSERC, NSF, and Yale University.

7 Appendix: A Glossary of Symbols

A^{vf} An area of the visual field corresponding to an area A^c of primary visual cortex.

A^c An area of primary visual cortex corresponding to an area A^{vf} of visual field.

α_i Lower bound on the domain of a piecewise-linear amplifier function $g_i(u_i)$.

$\alpha_{i,j}$ Beginning of jth piecewise linear segment of amplifier function $g_i(u_i)$.

β_i Upper bound on the domain of a piecewise-linear amplifier function $g_i(u_i)$.

$\alpha_{i,j+1} = \beta_{i,j}$ beginning of $j+1$th piecewise linear segment of amplifier function $g_i(u_i)$.

c_i Input capacitance of amplifier i.

C The total set of model neuronal cliques.

$|C|$ The number of cliques in the set C.

C^p An individual clique of model neurons belonging to the total set of cliques C.

$C - C^p$ The set of cliques C minus the clique C^p.

$C(i,j)$ The number of ways in which j items can be chosen from a set of i items: "i choose j." $C(i,j) = i!/(j!(i-j)!)$.

$\delta_{i,j}$ The constant used in the definition of the jth piecewise-linear segment of amplifier i.

E A set of model neurons which is initially activated with a bias current. This corresponds to a set of cortical neurons which spike initially in response to lower-level afferent stimulation.

$E(X)$ The expected value of the random variable X.

η_i^l An upper bound (sufficient) condition (based on T_{max}) on $|S(i)|$ for a model neuron i not to belong to the self-excitatory set S.

η_i^u An upper bound necessary condition on $|S(i)|$ (based on T_{min}) for a model neuron i not to belong to the self-excitatory set S.

η^l The minimum over all η_i^l.

f The dendritic fan-in of a model neuron.

g_i The ith piecewise-linear amplifier. Corresponds to a single model neuron.

$\gamma_{i,j}$ Coefficient used in the definition of the jth piecewise-linear segment of amplifier i.

h The number of lines per degree of orientation which can be discriminated by hyperacuity. For example if one can discriminate two line orientations 1/6 deg apart, then $h = 6$.

M The number of model neurons in a clique.

N The number of model neurons corresponding to the cortical area A^c.

R_i Inverse of model neuron i's membrane conductance plus synaptic conductance.

ρ^i Model neuron i's membrane resistance.

S A self-excitatory set of model neurons, i.e. a set of neurons sufficiently interconnected to drive themselves to saturated feedback levels.

S^i A completely interconnected subset of a self-excitatory set S.

$S(i)$ The set of amplifiers j (model neurons) in a self-excitatory set S which have nonzero connectivity T_{ij} to an amplifier i.

$|S(i)|$ The size of the set $S(i)$.

T_{ij} The conductance from amplifier j to amplifier i.

$T_{\max}$ The maximum over all T_{ij}.

$T_{\min}$ The minimum over all T_{ij}.

T_μ The expected value of T_{ij}.

u_i The input voltage to amplifier i.

V_i The output voltage of amplifier i.

ξ_i^l A lower bound on $|S(i)|$ for a model neuron i to belong to the self-excitatory set S based on the max conductance (Sec. 3.1).

ξ_i^u A lower bound condition on $|S(i)|$ for a model neuron i to belong to the self-excitatory set S based on the min conductance.

ξ^u The maximum over all ξ_i^u.

References

[1] Abbott, L., van Vreeswijk, C., 1993. Asynchronous states in networks of pulse-coupled oscillators. *Phys. Rev. E* 48, 1483 - 1490.

[2] Abeles, M. *Corticonics*, 1991, Cambridge University Press, New York.

[3] Albus, K. 1975. A quantitative study of the projection area of the central and the paracentral visual field in area 17 of the cat. *Exp. Brain Res*, **24**, 159-179 (Part I), 181-202 (Part II).

[4] Alpern, M. 1962. Types of movement. In: *The Eye, Vol. 3*, (H. Davson, ed.), 63-151. Academic Press, New York.

[5] Amari, S. 1989. Characteristics of sparsely encoded associative memory. *Neural Networks*, **2**, 45-457.

[6] Amit, D. J., H. Gutfreund, and H. Sompolinsky. 1987. Information storage in neural networks with low levels of activity. *Physical Review A*, **35**, 2293-2303.

[7] Amit, D. J. 1989. *Modeling Brain Function: the World of Attractor Neural Networks*, Cambridge University Press, Cambridge, England.

[8] Artola, A., S. Bröcher, and W. Singer. 1990. Different voltage-dependent thresholds for inducing long-term depression and long-term potentiation in slices of rat visual cortex. *Nature*, **347**, 69-72.

[9] Barlow, H. B. 1979. Reconstructing the visual image in space and time. *Nature*, **279**, 189-190.

[10] Barlow, H. B. 1983. Understanding natural vision. In: *Physical and Biological Processing of Images* (eds. O. J. Braddick and A. C. Sleigh), 2-14, Springer-Verlag, New York.

[11] Bishop, P. O., J. S. Coombs, and H. Henry. 1971. Responses to visual contours: spatio-temporal aspects of excitation in the receptive fields of simple striate neurones. *J. Physiol.*, **219**, 625-657.

[12] Bishop, P. O., J. S. Coombs, and H. Henry. 1973. Receptive fields of simple cells in the cat striate cortex. *J. Physiol.*, **231**, 31-60.

[13] Bishop, P. O., B. Dreher, and H. Henry. 1972. Simple striate cells: comparison of responses to stationary and moving stimuli. *J. Physiol.*, **227**, 15-17P.

[14] Braitenberg, V., 1974. Thoughts on the cerebral cortex, *J. Theor. Biol.* 46, 421 - 447.

[15] Braitenberg, V., 1978. Cell assemblies in the cerebral cortex, in R. Heim, G. Palm (eds.), *Theoretical Approaches to Complex Systems*, Lecture Notes in Biomathematics (21), Springer, New York, 171 - 188.

[16] Braitenberg, V., 1985. Charting the visual cortex, in A. Peters and E. Jones (eds), *Cerebral Cortex Vol. 3: Visual Cortex*, Plenum Press, New York, 379 - 414.

[17] Braitenberg, V. and Schuez, A., 1991. Anatomy of the Cortex. Statistics and Geometry. Springer, Berlin.

[18] Bullier, J., M. J. Mustari, and G. H. Henry. 1982. Receptive-field transformations between LGN neurons and S-cells of cat striate cortex. *J. Neurophysiology*, **47**, 417-438.

[19] Callaway, E. M. and L. C. Katz. 1990. Emergence and refinement of clustered horizontal connections in cat striate cortex. *J. Neurosci.*, **10**, 1134-1153.

[20] Calvin, W. H. 1978. Setting the pace and pattern of discharge: do CNS neurons vary their sensitivity to external inputs via their repetitive firing processes? *Federation Proceedings*, **37**, 2165-2170.

[21] Cohen, M. A. and S. Grossberg. 1983. Absolute stability of global pattern formation and parallel memory storage by competitive neural networks. *IEEE Trans. Sys. Man Cyber.*, **13**, 815-826.

[22] De Valois, R. L., E. W. Yund, and N. Hepler. 1982. The orientation and direction selectivity of cells in macaque visual cortex. *Vision Res.*, **22**, 531-544.

[23] Dobbins, A., S. W. Zucker, and M. S. Cynader. 1987. Endstopping in the visual cortex as a substrate for calculating curvature. *Nature*, **329**, 438-441.

[24] Douglas, R. J., Koch, C., Mahowald, M., K. A. C. Martin, and H. Suarez. 1995. Recurrent excitation in neocortical circuits. *Science*, **269**, 981 - 985

[25] Douglas, R. J., K. A. C. Martin, and D. Whitteridge. 1988. Selective responses of visual cortical cells do not depend on shunting inhibition. *Nature (London)*, **332**, 642-644.

[26] Douglas, R. J., K. A. C. Martin, and D. Whitteridge. 1989. A canonical microcircuit for neocortex. *Neural Computation*, **1**, 480-488.

[27] Douglas, R. J. and K. A. C. Martin. 1990. Neocortex. In: *The Synaptic Organization of the Brain, Third Edition* (ed. G. M. Shepherd), 389-438. Oxford University Press, New York.

[28] Douglas, R. J. and K. A. C. Martin. 1991. Opening the grey box. *Trends in Neuroscience*, **14**, 286-293.

[29] Douglas, R. J. and K. A. C. Martin. 1992. Exploring cortical microcircuits: a combined physiological and computational approach. In: *Single Neuron Computation, Neural Nets: Foundations to Applications (Ser.)*, (T. McKenna, J. Davis, and S. F. Zornetzer, eds.), 381-412, Academic Press, New York.

[30] Eckhorn, R., R. Bauer, W. Jordan, M. Brosch, W. Kruse, M. Munk, and H. J. Reitboeck. 1988. Coherent Oscillations: A mechanism of feature linking in the visual cortex? *Biol. Cybern.*, **60**, 121-130.

[31] Ferster, D. and S. Lindström. 1983. An intracellular analysis of geniculo-cortical connectivity in area 17 of the cat. *J. Physiol*, *342*, 181-215.

[32] Fisher, S., Zucker, S.W., and Carew, T.J., 1997. Use-dependent enhancement of frequency facilitation at L30 inhibitory synapes in Aplysia, *Soc. Neurosci. Abstracts*

[33] Freund, T. F., K. A. C. Martin, P. Somogyi, and D. Whitteridge. 1985. Innervation of cat areas 17 and 18 by physiologically identified X- and Y-type thalamic afferents. II. Identification of postsynaptic targets by GABA immunochemical and Golgi impregnation. *J. Comp. Neurol.*, **242**, 275-291.

[34] Garey, M. R. and Johnson, D. S. 1979. *Computers and Intractability.* W. H. Freeman, San Francisco.

[35] Georgopoulos, A. P., J. T. Lurito, M. Petrides, A. B. Schwartz, and J. T. Massey. 1989. Mental rotation of the neuronal population vector. *Science*, **243**, 234-236.

[36] Gilbert, C. D. and Wiesel, T. N. 1979. Morphology and intracortical projections of functionally characterized neurones in cat visual cortex. *Nature.* **280**, 120-125.

[37] Gilbert, C. D. and Wiesel, T. N. 1983. Clustered intrinsic connections in cat visual cortex. *J. Neurosci.*. **3**, 1116-1133.

[38] Gilbert, C. D. and Wiesel, T. N. 1989. Columnar specificity of intrinsic horizontal and corticocortical connections in cat visual cortex. *J. Neurosci.*. **9**, 2432-2442.

[39] Gilbert, C. D. and Wiesel, T. N. 1990. The influence of contextual stimuli on the orientation selectivity of cells in primary visual cortex of the cat. *Vision Res.*, **30**, 1689-1701.

[40] Gopalsamy, K., and He, X. 1994. Stability in asymmetric Hopfield nets with transmission delays. *Physica D*, 76, 344 - 358.

[41] Gray, C. M. and W. Singer. 1989. Stimulus-specific neuronal oscillations in orientation columns of cat visual cortex. *Proc. Natl. Acad. Sci. USA*, **86**, 1698-1702.

[42] Gray, C. M., P. König, A. K. Engel, and W. Singer. 1989 Oscillatory responses in cat visual cortex exhibit inter-columnar synchronization which reflects global stimulus properties. *Nature*, **338**, 334-337.

[43] Harth, E., Csermely, T., Beek, B., and Lindsay, R.D., 1970. Brain functions and neural dynamics. *J. Theor. Biol.* 26, 93 - 120.

[44] Hebb, D.O., 1949, *The Organization of Behaviour*, Wiley, New York.

[45] Heller, J., Hertz, J., Kjaer, T., and Richmond, B. 1995. Information flow and temporal coding in primate pattern vision, *J. Computational Neuroscience*, 2, 175 - 193.

[46] Henry, G. H. 1977. Receptive Field Classes of Cells in the Striate Cortex of the Cat. *Brain Research*, **133**, 1-28.

[47] Henry, G. H., A. R. Harvey and J. S. Lund. 1979. The afferent connections and laminar distribution of cells in the cat striate cortex. *J. Comp. Neurol.*, **187**, 725-744.

[48] Hirsch, M. W. and S. Smale. 1974. *Differential Equations, Dynamical Systems, and Linear Algebra*, Academic Press, New York.

[49] Hopfield, J. J. 1984. Neurons with graded response have collective computational properties like those of two-state neurons. *Proc. Natl. Acad. Sci. USA*, **81**, 3088-3092.

[50] Hopfield, J. J. and D. W. Tank. 1985. "Neural" computation of decisions in optimization problems. *Biol. Cybern.*, **52**, 141-152.

[51] Horton, J. C., L. R. Dagi, E. P. McCrane, and F. M. de Monasterio. 1990. Arrangement of ocular dominance columns in human visual cortex. *Arch Ophthalmol*, **108**, 1025-1031.

[52] Hubel, D. H. and T. N. Wiesel. 1962. Receptive fields, binocular interaction and functional architecture in the cat's visual cortex. *J. Physiol.*, **160**, 106-154.

[53] Hubel, D. H. and T. N. Wiesel. 1968. Receptive fields and functional architecture of monkey striate cortex. *J. Physiol.*, **195**, 215-243.

[54] Hubel, D. H. and T. N. Wiesel. 1977. Ferrier Lecture. Functional architecture of macaque monkey visual cortex. *Proc. R. Soc. Lond. B.*, **198**, 1-59.

[55] Hummel, R.A., and Zucker, S.W., 1983. On the foundations of relaxation labeling processes, *IEEE Trans. Pattern Analysis and Machine Intelligence*, **PAMI-5**, 267-287.

[56] König, P., and Engel, A., 1995. Correlated firing in sensory-motor systems. *Current Opinion in Neurobiology*, **5**, 511 - 519.

[57] Krüger, J. and J. D. Becker. 1991. Recognizing the visual stimulus from neuronal discharges. *Trends in Neuroscience*, **14**. 282-286.

[58] Lehky, S. R. and T. J. Sejnowski. 1990. Neural model of stereoacuity and depth interpolation based on a distributed representation of stereo disparity. *J. Neuroscience*, **10**, 2281-2299.

[59] Löwel, S., and Singer, W., 1992. Selection of intrinsic horizontal connections in the visual cortex by correlated neuronal activity. *Science*, **255**, 209 - 212.

[60] Marcus, C., Waugh, F., Westervelt, R., 1990. Associative memory in an analog iterated-map network. *Phys. Rev. A* 41(6), 3355 - 3364.

[61] Marcus, C., Westervelt, R., 1989. Dynamics of iterated-map networks. *Phys. Rev. A* 40(1), 501 - 504.

[62] Martin, K. A. C. 1984. Neuronal circuits in cat striate cortex. In: *Cerebral Cortex, Vol. 2: Functional Properties of Cortical Cells*, (E. G. Jones and A. Peters, eds.), 241-284, Plenum Press, New York.

[63] McCormick, D. A., B. W. Connors, J. W. Lighthall, and D. A. Prince. 1985. Comparative electrophysiology of pyramidal and sparsely spiny stellate neurons of the neocortex. *J. Neurophysiol.*, **54**, 782-806.

[64] McCormick, D. A. 1990. Membrane properties and neurotransmitter actions. In: *The Synaptic Organization of the Brain*, (G. M. Shepherd, ed.), 32-66. Oxford University Press, New York.

[65] McClurkin, J., Gawne, T., Optical, L., and Richmond, B., 1991. Lateral geniculate neurons in behaving primates. II. Encoding of visual information in the temporal shape of the response. *J. Neurophys.* 66, 794 - 808.

[66] Meister, M., 1996. Multineuronal codes in retinal signaling. *Proc. Nat. acad. Sci (USA)*, 93, 609 - 614.

[67] Michel, A., Farrell, J., and Porod, W., 1988. Stability results for neural networks. In D. Z. Anderson: Neural Information Processing Systems. American Institute of Physics, New York, 554 - 563.

[68] Miller, D. A. and S. W. Zucker. 1991. Copositive-plus Lemke algorithm solves polymatrix games. *Operations Research Letters*, **10**, 285-290.

[69] Miller, D. A. and S. W. Zucker. 1992. Efficient simplex-like methods for equilibria of nonsymmetric analog networks. *Neural Computation*, **4**, 167-190.

[70] Miller, D. A. and S. W. Zucker. 1998. Cliques, Computation, and Computational Tractability. *Pattern Recognition*, to be published; *Workshop on Energy Minimization Methods in Computer Vision and Pattern Recognition*, Venice, May 1997, Pelillo and Hancock (eds), Lecture Notes in Computer Science 1223, Springer Verlag, New York, 1997.

[71] Miller, K. D., J. B. Keller, and M. P. Stryker. 1989. Ocular dominance column development: analysis and simulation. *Science*, **245**, 605-615.

[72] Moore, E. F. and C. E. Shannon. 1956. Reliable circuits using less reliable relays. *J. Franklin Inst.*, **262**, 191-208, 281-297.

[73] Nelken, I., 1988. Analysis of the activity of single neurons in stochastic settings. *Biol. Cybern.* 59, 201 - 215.

[74] Palm, G., 1980. On associative memory. *Biol. Cybern.* 36, 19 - 31.

[75] Palm, G. 1981. On the storage capacity of associative memory with randomly distributed storage elements. *Biol. Cybern.*, **39**, 125-127.

[76] Palm, G. 1982. *Neural Assemblies: An alternative approach to artificial intelligence.* Springer, Berlin, 1982.

[77] Palm, G., 1993. Cell assemblies, coherence and cortico-hippocampal interplay. *Hippocampus*, 3, 219 - 225.

[78] Palm, G., Aertsen, A., 1986. (eds) Brain Theory. Springer, Berlin.

[79] Peters, A. 1987. Number of neurons and synapses in the primary visual cortex. In: *Cerebral Cortex, Vol. 6: Further Aspects of Cortical Functions Including Hippocampus*, (E. G. Jones and A. Peters, eds.), 267-294, Plenum Press, New York.

[80] Peters, A. and C. Sethares. 1991. Organization of pyramidal neurons in area 17 of monkey visual cortex. *J. Comp. Neurol.*, **306**, 1-23.

[81] Rockland, K. S., and J. S. Lund. 1982. Widespread periodic intrinsic connections in the tree shrew visual cortex. *Science*, **215**, 1532-1534.

[82] Rockland, K. S. and J. S. Lund. 1983. Intrinsic laminar lattice connections in primate visual cortex. *J. Comp. Neurol.*, **216**, 303-318.

[83] Rockland, K. S., J. S. Lund, and A. L. Humphrey. 1982. Anatomical banding of intrinsic connections in striate cortex of tree shrews (tupaia glis). *J. Comp. Neurol.*, 209, 41-58.

[84] Schiller, P. H., B. L. Finlay, and S. F. Volman. 1976a. Quantitative studies of single-cell properties of monkey striate cortex. I. Spatio-temporal organization of receptive fields. *J. Neurophysiology*, **6**, 1288-1319.

[85] Schiller, P. H., B. L. Finlay, and S. F. Volman. 1976b. Quantitative studies of single-cell properties of monkey striate cortex. II. Orientation specificity and ocular dominance. *J. Neurophysiology*, **6**, 1320-1333.

[86] Schiller, P. H., B. L. Finlay, and S. F. Volman. 1976c. Quantitative studies of single-cell properties of monkey striate cortex. III. Spatial frequency. *J. Neurophysiology*, **6**, 1334-1351.

[87] Segev, I., J. W. Fleshman, and R. E. Burke. 1989. Compartmental models of complex neurons. In: *Methods in Neuronal Modeling: From Synapses to Networks*, C. Koch and I. Segev, eds. MIT Press, Cambridge, Mass.

[88] Sejnowski, T. J. 1981. Skeleton filters in the brain. In: *Parallel Models of Associative Memory* (G. E. Hinton and J. A. Anderson, eds.), Lawrence Erlbaum Assoc., Hillsdale, N. J.

[89] Shimojo, S., E. E. Birch, J. Gwiazda, and R. Held. 1984. Development of vernier acuity in infants. *Vision Res.*, **24**, 721-728.

[90] Softky, W., and Koch, C. 1992 Cortical cells should fire regularly, but do not. *Neural Computation*, **4**, 643 - 645.

[91] Singer, W. 1990. The formation of cooperative cell assemblies in the visual cortex. *J. exp. Biol.*, **153**, 177-197.

[92] Traub, R., Whittington, M., Stanford, I., and Jerrerys, J. 1996. A mechanism for generation of long-range synchronous fast oscillations in the cortex. *Nature*, 383, 621 - 624.

[93] Treves, A., Mean-field analysis of neuronal spike dynamics. 1993. *Network* 4, 259 - 284.

[94] Ts'o, D. Y., R. Frostig, E. E. Lieke, A. Grinvald. Functional organization of primate visual cortex revealed by high resolution optical imaging. 1990. *Science*, **249**, 417-420.

[95] Tsodyks, M., Mitkov, I., and Sompolinsky, H., 1993. Pattern of synchrony in inhomogeneous networks of oscillators with pulse interactions. *Phys. Rev. Let.*, **71**, 1280 - 1283.

[96] Varela, J., Sen, K., Gibson, J., Fost, J., Abbott, L.F., and Nelson, S., 1997. A quantitative description of short-term plasticity at excitatory synapses in layer 2/3 of rat primary visual cortex. *J. Neurosci.*, **17**, 7926 - 7940.

[97] Victor, J., 1987. The dynamics of the cat retinal X-cell centre. *J. Physiol. (London)*, 386, 219 - 246.

[98] Waugh, F., Marcus, C., and Westervelt, R., 1991. Reducing neuron gain to eliminate fixed-point attractors in analog associative memory. *Phys. Rev. A*, 43(6), 3131 - 3142.

[99] Wennekers, T., Sommer, F., Palm, G., 1995. Iterative retrieval in associative memories by threshold control of different neural models. *Proc. Workshop on Supercomputers in Brain Research*, (Hermann, H.J., ed.), World Scientific.

[100] Westheimer, G. 1982. The spatial grain of the perifoveal visual field. *Vision Res.*, **22**, 157-162.

[101] Westheimer, G. 1990. The grain of visual space. *Cold Spring Harbor Symposia on Quantitative Biology, Vol. LV*, 759-763.

[102] Westheimer, G. and S. P. McKee. 1975. Visual acuity in the presence of retinal-image motion. *J. Opt. Soc. Am.*, **65**, 847-850.

[103] Westheimer, G. and S. P. McKee. 1977. Spatial configurations for visual hyperacuity. *Vision Res.*, **17**, 941-947.

[104] Wiesel, T. N. and D. H. Hubel. 1970. In *Genetic and Experiential Factors in Perception* (ed. R. A. McCleary). Scott, Foresman and Co., Glenview, Illinois.

[105] Willshaw, D. J., O. P. Buneman, and H. C. Longuet-Higgins. 1969. Non-holographic associative memory. *Nature*, **222**, 960-962.

[106] Willshaw, D. J. and H. C. Longuet-Higgins. 1970. Associative memory models. In *Machine Intelligence, Vol. 5* (B. Meltzer and D. Michie, eds.), 351-359, Edinburgh U. Press, Edinburgh, U.K.

[107] Wilson, H. R., D. Levi, L. Maffei, J. Rovamo, and R. DeValois. 1990. The Perception of Form: Retina to Striate Cortex. In: *Visual Perception* (eds. L. Spillman and J. S. Werner), 231-272, Academic Press, New York.

[108] Winograd, S. and J. D. Cowan. 1963. *Reliable Computation in the Presence of Noise*, MIT Press, Cambridge, Mass.

[109] Wörgötter, F. and C. Koch. 1991. A detailed model of the primary visual pathway in the cat: comparison of afferent excitatory and intracortical inhibitory connection schemes for orientation selectivity. *J. Neuroscience*, **11**, 1959-1979.

[110] Zucker, S. W., A. Dobbins, and L. Iverson. 1989. Two stages of curve detection suggest two styles of visual computation. *Neural Comp.*, **1**, 68-81.